REVIEW

Glucose Biosensing

NANO · MICRO
smal
www.small-journal.com

Check for updates

Peroxidase-Like Activity of Smart Nanomaterials and Their Advanced Application in Colorimetric Glucose Biosensors

Xigui Liu, Danlian Huang,* Cui Lai,* Lei Qin, Guangming Zeng, Piao Xu, Bisheng Li, Huan Yi, and Mingming Zhang

Diabetes is a dominating health issue with 425 million people suffering from the disease worldwide and 4 million deaths each year. To avoid further complications, the diabetic patient blood glucose level should be strictly monitored despite there being no cure for diabetes. Colorimetric biosensing has attracted significant attention because of its low cost, simplicity, and practicality. Recently, some nanomaterials have been found that possess unexpected peroxidase-like activity, and great advances have been made in fabricating colorimetric glucose biosensors based on the peroxidase-like activity of these nanomaterials using glucose oxidase. Compared with natural horseradish peroxidase, the nanomaterials exhibit flexibility in structure design and composition, and have easy separation and storage, high stability, simple preparation, and tunable catalytic activity. To highlight the significant progress in the field of nanomaterial-based peroxidase-like activity, this work discusses the various smart nanomaterials that mimic horseradish peroxidase and its mechanism and development history, and the applications in colorimetric glucose biosensors. Different approaches for tunable peroxidase-like activity of nanomaterials are summarized, such as size, morphology, and shape; surface modification and coating; and metal doping and alloy. Finally, the conclusion and challenges facing peroxidase-like activity of nanomaterials and future directions are discussed.

1. Introduction

Diabetes, a clinical chronic illness attributed to the increase of glucose level, appears because of the malfunction of pancreatic β cells responsible for insulin production which tightly adjust the levels of glucose in the blood.[1,2] In diabetic patients, the increased glucose level possesses major and serious life-threatening illnesses such as nervous, cordis,

nephric, cerebral, peripheral vessel, and ophthalmic illnesses.[3,4] Diabetes is a dominating health issue inducing 425 million people suffering from diabetes worldwide and 4 million deaths each year.[5,6] According to some statistics, the global number of diabetic patients will be one and half times the existing patients.[7,8] In order to avoid further complications, the diabetic patient blood glucose level should be strictly monitored in spite of there being no cure for diabetes.[9,10] Because of the increasing attention about this disease, the fabrication of sensitive and accurate blood glucose testing devices have become a potential trend for continuous monitoring of glucose in blood.[11,12] Moreover, the monitoring of food and ecological, development of sustainable and renewable energy, and clinical diagnosis urgent need development of glucose detection devices.[13,14] These promote a widespread mercantile and academic efforts to develop glucose biosensors with good reliability, excellent sensitivity and selectivity, low cost, and fast response.[15–17]

Owing to its practicality, simplicity, and low cost, colorimetric biosensing has drawn increasing concerns.[18–20] Conversion of target analytes into color changes emerges as a key challenge for colorimetric biosensing.[21–23] Colorimetric biosensing does not need complicated and costly apparatus, and can be used in point-of-care diagnosis and on-site analysis since the color changes can be read by the unaided eye.[24–27] Peroxidase activity shows an enormous potential for actual application and has been applied to the degradation of pollutants or as detection kits.[28,29] The ability to catalyze the oxidation of organic substrates to generate a color change and reduce their toxicity contribute to these extensive applications. The catalytic activity of peroxidase can be evaluated by peroxidase substrates such as 3,3′,5,5′-tetramethylbenzidine (TMB), 2,2′-azino-bis(3-ethylbenzothiazoline-6-sulfonic acid) (ABTS), o-phenylenediamine (OPD), and diazoaminobenzene (DAB). These substrates display a distinguishable color change when catalytic oxidized by peroxidase in the presence of hydrogen peroxide (H_2O_2). The catalytic color reaction supplies another tool for colorimetric biosensing. Transforming the glucose into H_2O_2 and gluconic acid in the presence of glucose oxidase (GOx) is the mainly basis of colorimetric detection of glucose. Then, the generated

Dr. X. Liu, Prof. D. Huang, Prof. C. Lai, Dr. L. Qin, Prof. G. Zeng,
Dr. P. Xu, Dr. B. Li, Dr. H. Yi, M. Zhang
College of Environmental Science and Engineering
Hunan University
Changsha, Hunan 410082, China
E-mail: huangdanlian@hnu.edu.cn; laicui@hnu.edu.cn
Dr. X. Liu, Prof. D. Huang, Prof. C. Lai, Dr. L. Qin, Prof. G. Zeng,
Dr. P. Xu, Dr. B. Li, Dr. H. Yi, M. Zhang
Key Laboratory of Environmental Biology and Pollution Control
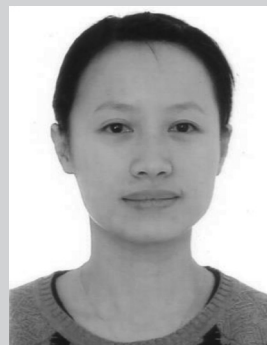Hunan University
Changsha, Hunan 410082, China

H_2O_2 catalytic oxidation by peroxidase in the presence of TMB, ABTS, DAB, and OPD leads to the generation of a colored product that can be used for colorimetric detection of glucose.

Natural horseradish peroxidase (HRP) has been used to catalyze H_2O_2 for a long time. However, the natural peroxidase suffers some drawbacks: a) the activity of natural peroxidase is easily denatured by digestive proteases or environmental changes and are unstable in natural environment, and b) the purification, preparation, and storage is usually costly and time-consuming.[16] To overcome these shortcomings, great efforts have been committed to develop peroxidase mimetics. Among them, many peroxidase mimetics, such as porphyrin, hemin, cyclodextrin, and hematin, have been successfully developed and applied to H_2O_2 detection.[30,31] Since it was reported first that Fe_3O_4 magnetic nanoparticles (MNPs) possessed intrinsic peroxidase-like activity in 2007,[32] thus opening the door for the development of nanomaterial-based peroxidase-like. Some nanomaterials, such as MNPs (Fe_3O_4 MNPs, $CoFe_2O_4$ MNPs, $ZnFe_2O_4$ MNPs, $NiFe_2O_4$ MNPs, $MgFe_2O_4$ MNPs, etc.), carbon nanomaterials (graphene oxide (GO), fullerene-C_{60}, carbon nanodots, carbon nitride dots, single-walled carbon nanotubes (SWCNTs), etc.), metal oxide nanomaterials (Co_3O_4 NPs, CeO_2 NPs, CeO_2 nanorods (CeO_2 NRs), MnO_2 nanosheets (MnO_2 NSs), MnO_2 nanowires (MnO_2 NWs), CuO NPs, VO_2 NPs, VO_2 nanofibers, VO_2 nanosheets (VO_2 NSs), VO_2 nanorods (VO_2 NRs), V_2O_3 NPs, V_2O_5 nanowires (V_2O_5 NWs)), metal sulfide nanomaterials (ZnS NPs, MoS_2 NPs, MoS_2 nanosheets (MoS_2 NSs), FeS nanosheets (FeS NSs) etc.), metal nanomaterials (Au NPs, Ag NPs, gold clusters, rhodium NPs, Pt nanotubes (Pt NTs), Au@Ag NPs, etc.), and nanocomposites (GO–Fe_3O_4 nanocomposite, Cu–Ag/rGO nanocomposite, MoS_2/GO nanocomposite, etc.), are found to possess intrinsic peroxidase-like activity. Based on these developed intrinsic peroxidase-like activity of nanomaterials, a peroxidase-like activity of nanomaterial-based biosensor has appeared as an important colorimetric means for the detection of glucose. Compared to HRP, nanomaterials represent ideal candidates for traditional peroxidase mimetics, showing high stability and resist rigorous reaction conditions. Furthermore, they possess other advantages such as tunable catalytic activities, flexibility in structure composition and design, and controlled preparation at low cost.

Glucose detection is of critical role in the improvement of human life quality and plays a significant importance in food detection and clinical diagnosis.[33] Recently, many authoritative and excellent reviews have been reported the fabrication of electrochemical glucose biosensor.[34–36] Because there is a rapid growing in the assembly of colorimetric glucose biosensor based on peroxidase-like activity of nanomaterials, it was first reported by Wei et al. using Fe_3O_4 MNPs as peroxidase-like for colorimetric detection of glucose in 2008.[37] Hence, we summarized the current research literatures on colorimetric biosensor for glucose detection by employing peroxidase-like activity of nanomaterials. To highlight the recent advances in nanomaterial-based peroxidase-like, this review discusses the various nanomaterials that have been unveiled to mimic HPR. The development history, mimic HPR and its mechanism, and application for colorimetric glucose biosensor are concluded (see **Figure 1**). Moreover, different approaches for tunable peroxidase-like of nanomaterials are summarized. Finally, the conclusion and challenges

Xigui Liu received his B.S. degree in the College of Resources and Environment, Jinan University, in 2014. He is currently in the second year of his Ph.D. in Hunan University under the supervision of Prof. Danlian Huang. His major research focus is on the fabrication and application of nanomaterials in environmental detection and control.

Danlian Huang obtained her Ph.D. in Environmental Engineering in Hunan University in 2011. In 2015, she was promoted to Full Professor of Environmental Engineering at the same University. Her research focused on the remediation of soils polluted by organic compounds and heavy metals.

Cui Lai graduated from the College of Environmental Science and Engineering of Hunan University in 2013 and received her Ph.D. degree in Environmental Science. She joined Prof. Guangming Zeng's group at Hunan University after completing her Ph.D. degree. Her main research interests are the development and environmental application of functional nanomaterials.

facing peroxidase-like of nanomaterials and future directions are discussed.

2. Peroxidase-Like Activity of Nanomaterials

Nanomaterials with enzyme-like characteristics have got increasingly attention in nanoresearch.[38–40] To our best knowledge, the progress and achievements of the nanomaterials-based nanozymes have been thoroughly reviewed in previous literatures.[41–44] These reviews all introduced different enzyme-like activity of nanomaterials and their different applications: enzyme-like characteristics such as catalase-like activity, superoxide oxidase-like activity, ribonuclease-like activity, oxidase-like activity, and peroxidase-like activity[43]; applications such as anti-inflammatory effects, antioxidants, neuroprotection, promotion
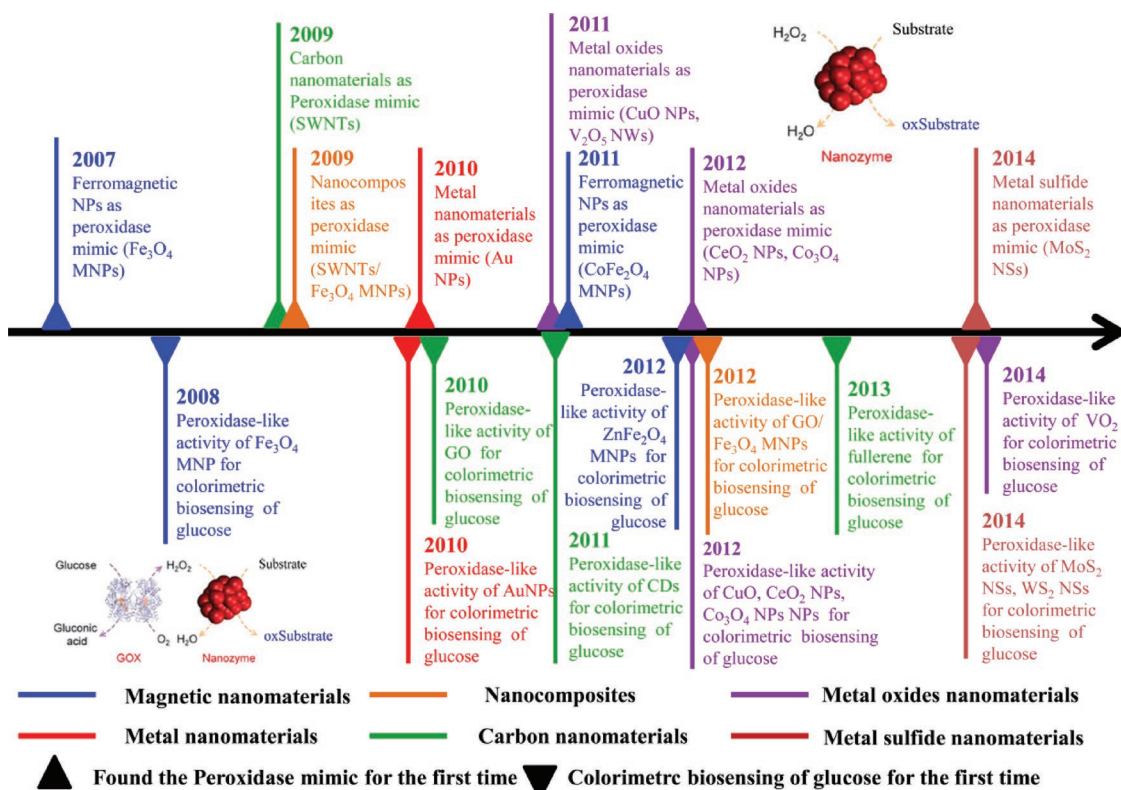
Figure 1. A brief timeline for the development of peroxidase-like activity of smart nanomaterials and its application for colorimetric glucose biosensor.

of stem cell growth, H_2O_2 detection, glucose detection, DNA detection, immunoassays, and pollutant removal. However, none of them introduces the peroxidase-like activity of nanomaterials and their application for colorimetric glucose biosensor in detail. Besides, there is no review summarized the mechanism of nanomaterials which mimic peroxidase catalytic activity with systematic and detailed. More importantly, most of these reviews were published before 2014, which implies that the cited papers were introduced before 2014. In the past 4 years, many new excellent papers have been reported. Therefore in this review, we detail the peroxidase-like activity of nanomaterials, and its catalytic mechanism and application for colorimetric glucose biosensor. The peroxidase-like activity of nanomaterials is classified into six parts: magnetic nanomaterials, carbon nanomaterials, metal oxide nanomaterials, metal sulfide nanomaterials, metal nanomaterials, and nanocomposites.

2.1. Magnetic Nanomaterials

The intrinsic peroxidase-like activity of magnetic nanomaterials (Fe_3O_4 MNPs) was first reported by Yan's group in 2007.[32] In Yan's work, the substrate TMB can be oxidized to the blue-colored product by three different sizes (30, 50, and 300 nm) of Fe_3O_4 MNPs in the presence of H_2O_2 through mimicking the activity of HRP (**Figure 2**). Similarly, Fe_3O_4 MNPs can also oxidize other two detected substrates (OPD and DAB) to their corresponding colored products. Compared with HRP, Fe_3O_4 MNPs are much more robust as they remain their catalytic activity and retain stable after incubation at a wide pH range of 0–12 and temperatures

(4–90 °C). Furthermore, as a catalyst, Fe_3O_4 MNPs are highly effective, with a higher binding affinity for the substrate TMB compared with HRP. Moreover, under the same molar concentration of catalyst, Fe_3O_4 MNPs show a 40-fold higher level of activity than HRP (**Figure 3**). The catalytic mechanism of the peroxidase-like activity of Fe_3O_4 MNPs is dependent on Fe^{2+} and Fe^{3+} ions in solutions as the Fenton's reagents which catalyze the breakdown of H_2O_2 to produce hydroxyl (·OH) radical. Since the path-breaking research reported by Yan et al.,[32] a larger number of studies have paid close attention to imitating peroxidase activity with various nanomaterials and explore its potential applications. More importantly, the magnetic properties of the MNPs can potentially be used for recovery or recycling of the MNPs. Lately, MFe_2O_4 (M = Co, Zn, Mg, Ni, Cu, Mn) MNPs were also explored to possess intrinsic peroxidase-like.[45–50] The peroxidase-like catalytic activity of these MNPs may depend on Fe^{2+}, Fe^{3+}, and M^{2+} (M = Co, Zn, Mg, Ni, Cu, Mn) ions in solutions just like the Fenton's reagents which are known to catalyze the breakdown of H_2O_2 to generate ·OH.[51–53] Moreover, the Fe_3S_4 MNPs were also revealed to possess intrinsic peroxidase-like activity.[54]

In order to improve colloidal stability, high affinity toward the substrates, and catalytic activities of MNPs, a suitable surface modification and metal doping was also studied by many groups.[55–60] We discuss this in detail in Section 3.1.

2.2. Carbon Nanomaterials

Carbon-based nanomaterials, such as carbon nanotubes (CNTs),[61,62] graphene,[63,64] GO,[65] fullerene,[66] carbon nanodots
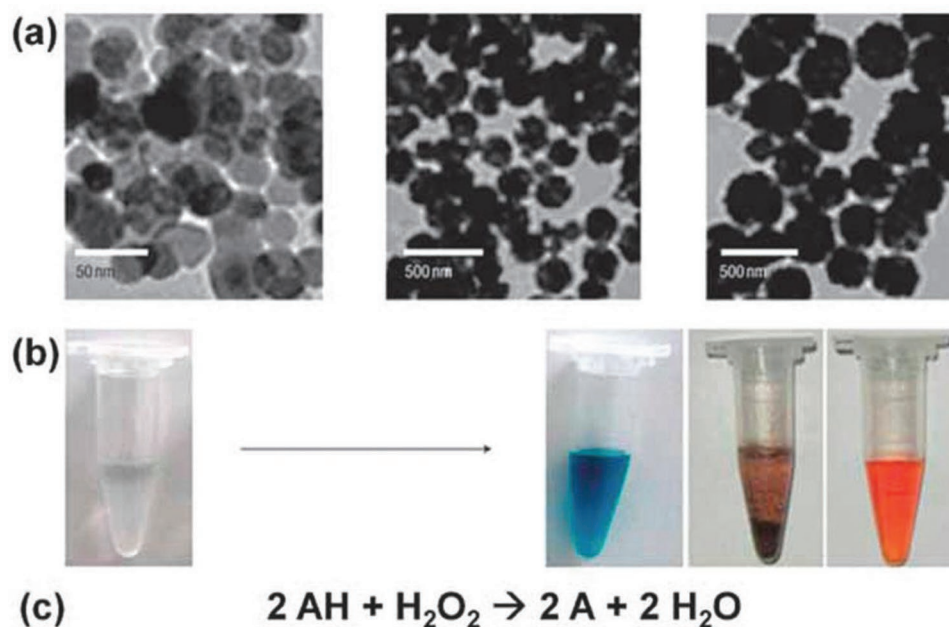
Figure 2. Fe_3O_4 MNPs as peroxidase-like to mimic peroxidase. a) TEM image of different sizes of Fe_3O_4 MNPs. b) Fe_3O_4 MNPs catalyze oxidize of substrates (TMB, DAB, and OPD) to generate corresponding colorimetric products in the presence of H_2O_2. c) The mechanism of catalysis by Fe_3O_4 MNPs. AH represents the substrate. Reproduced with permission.[43] Copyright 2007, Nature Publishing Group.

or carbon quantum dots,[67–71] carbon nitride dots,[72] graphite-like carbon nitrides (g-C_3N_4),[73,74] and graphene quantum dots (GQDs),[75,76] show great intrinsic peroxidase-like activity and applied to various applications. Carbon nanomaterials SWCNTs as peroxidase-like to mimic peroxidase was first reported by Song et al. in 2009.[62] They proved that the catalytic activity was attributed to SWCNTs instead of trace amount of metal catalysts. Following this study, Cui's study revealed that the activity of helical CNTs was affected by Fe content.[61] They found that higher content of Fe led to better catalytic activity. Simultaneously, they revealed that multiwalled carbon nanotubes (MWCNTs) had lower catalytic performance compared with helical CNTs; however, there was no direct comparison made between MWCNTs and helical CNTs, requiring significant systematic researches to compare the difference between these researches.

Carboxyl-modified graphene oxide (GO–COOH) was also revealed to possess intrinsic peroxidase activity by Song et al.[65] GO–COOH displays a lower affinity toward H_2O_2 compared to HRP (K_m, 0.214 mM for HRP vs 3.99 mM for GO–COOH), but a higher affinity toward TMB compared to HRP (K_m, 0.275 mM for HRP vs 0.0237 mM for GO–COOH) because of its high affinity toward organic substrates and very high surface-to-volume ratio. No catalytic activity was discovered at pH 7.0 in spite of the GO–COOH having intrinsic peroxidase-like activity, which may restrict their application under physiological conditions. Subsequently, hemin functionalized grapheme (graphene/hemin) synthesized as a peroxidase mimic was reported by Guo and co-workers for the first time.[64] The graphene/hemin hybrid nanosheets were composed through π–π interactions between hemin and graphene. The intrinsic peroxidase-like activity graphene/hemin was revealed by the transition of OPD, ABTS, and TMB to their corresponding colored product. Results showed that the intrinsic peroxidase-like activity graphene/hemin mainly originated from the hemin. The kinetics studies revealed the catalytic reaction of graphene/hemin hybrids showed a ping-pong mechanism, which was in accordance with HRP and other carbon-based nanomaterials. However, different from GO and CNTs, the graphene/hemin hybrids showed a lower affinity toward TMB but a higher affinity toward H_2O_2 than HRP, requiring further computational researches, as well as experimental to explain the difference.

A recent study[77] has been reported to understand the catalytic mechanism of nanocarbon-based artificial peroxidase (CNTs, graphene, GO and GQDs, etc.). By selectively inactivating the hydroxyl, carboxylic, or ketonic carbonyl groups and evaluating the catalytic activities of these graphene quantum dots derivatives, it was concluded that the $-C=O$ groups were the catalytically active sites, whereas the $O=C-O-$ groups acted as substrate-binding sites, and $-C-OH$ groups can inhibit the activity.

In 2009, Li et al. reported the intrinsic peroxidase-like activity of fullerene ($C_{60}[C(COOH)_2]_2$) for the first time.[66] The peroxidase-like catalytic mechanism of ($C_{60}[C(COOH)_2]_2$) is as follows: a) $C_{60}[C(COOH)_2]_2$ is π-rich and therefore can effectively adsorb TMB via π–π stacking interactions and the amino groups of TMB donated lone-pair electrons to carbon cage, which induce an increase of electron mobility and density in carbon cage, and b) the interface of hydrophilic moiety of carbon cage accelerates the electron transfer from carbon cage to H_2O_2.

g-C_3N_4, an analog of graphite, is an attractive 2D structure organic semiconductor material with a band gap of ≈2.7 eV.[78] Compared with inorganic semiconductors, g-C_3N_4 has shown many advantages such as chemical stability, low cost, is metal-free, environment friendly, and has tunable electronic

ADVANCED
SCIENCE NEWS
www.advancedsciencenews.com

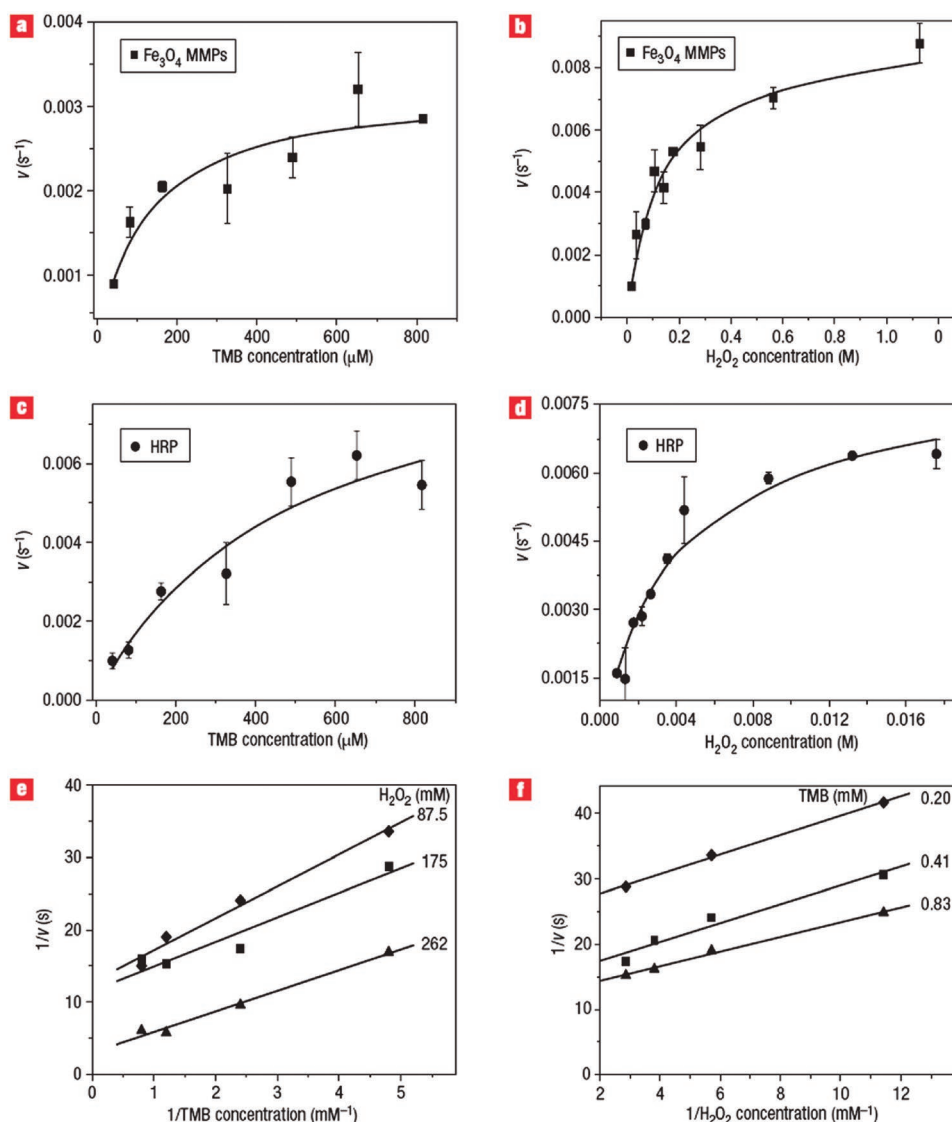NANO · MICRO
small
www.small-journal.com

Figure 3. Steady-state kinetic assay and catalytic mechanism of Fe_3O_4 MNPs as peroxidase mimic. Reproduced with permission.[32] Copyright 2013, The Royal Society of Chemistry.

structure.[79] Recent years have witnessed the widespread application of g-C_3N_4 in photocatalytic and photovoltaic fields.[80] The intrinsic fluorescence property of g-C_3N_4 also attributes itself to metal ion sensing and bioimaging applications. The peroxidase catalytic mechanism of g-C_3N_4 is as follows: TMB is absorbed on the surface of π-rich g-C_3N_4 through π–π stacking interactions. As a consequence, electron transfer from nitrogen atoms in TMB to g-C_3N_4 appears attribute to they close proximity, resulting in an increase in electron mobility and density in g-C_3N_4. This n-type doping of g-C_3N_4 increases its Fermi level, accordingly accelerating the electron transfer from g-C_3N_4 to H_2O_2.[73,74]

2.3. Metal Oxide Nanomaterials

The intrinsic peroxidase-like activity of metal oxides-based nanomaterials including copper oxide,[81–84] cerium oxide,[85–89] cobalt oxide,[90–93] manganese dioxide,[94,95] vanadium oxides (VO$_2$, V$_2$O$_3$, V$_2$O$_5$),[96–100] and nickel oxide[101] are widely explored. Chen et al. first reported the intrinsic peroxidase-like activity of copper oxide nanoparticles (CuO NPs) in 2011.[84] They found that the CuO NPs showed higher affinity to TMB than HPR and some other nanomaterials (i.e., Fe_3O_4 MNPs, GO–COOH, FeS NSs, etc.). The mechanism of peroxidase-like activity of CuO NPs is that CuO NPs can break up the O—O bond of H_2O_2 into two ·OH radical. Cubic cobalt oxide nanoparticles (Co$_3$O$_4$ NPs) found to possess dual intrinsic enzyme activities (i.e., peroxidase- and catalase-like activities) were first reported by Wang and co-workers in 2012.[93] The peroxidase mimicking activity of Co$_3$O$_4$ NPs was tested by catalytic oxidation of TMB in the presence of H_2O_2. Kinetics studies revealed that the Co$_3$O$_4$ NPs had lower affinity toward H_2O_2 but higher affinity toward TMB when compared with HRP. Interestingly different from other nanomaterials, the ability of electron

transfer between the substrate and H_2O_2 is responsible for the mechanism of the peroxidase-like activity of the Co_3O_4 NPs, not from $\cdot$OH radical generated. The peroxidase-like activity of cerium oxide nanoparticles (CeO_2 NPs) was first reported by Wang et al. in 2012.[85] Results showed that the CeO_2 NPs possessed peroxidase-like catalytic activity with a wide range of temperatures and pH values compared with natural enzymes. Simultaneously, kinetic analysis showed that the prepared CeO_2 NPs had a higher affinity toward TMB than natural enzyme HRP. The catalytic activity of CeO_2 NPs is mainly ascribed to the reversible switch between $Ce^{4+} \leftrightarrow Ce^{3+}$ and the presence of associated oxygen vacancies which induce the generation of $\cdot$OH. Simultaneously, Pirmohamed et al.[102] demonstrated that cerium oxide with high Ce^{4+}/Ce^{3+} ratios could act as catalase mimetics, which cause the decomposition of H_2O_2 to molecular oxygen (O_2). Therefore, the key to improve the peroxidase-like activity of cerium oxide is to adjust the Ce^{4+}/Ce^{3+} ratios and obtain more oxygen vacancies. The peroxidase-like activity of vanadium pentoxide nanowires (V_2O_5 NWs) was reported by Tremel' groups in 2011 for the first time.[99] V_2O_5 NWs show an intrinsic peroxidase catalytic activity toward substrates ABTS and TMB in the presence of H_2O_2. Results indicated that the V_2O_5 NWs had higher affinity toward those substrates than HPR. The proposed catalytic mechanism of V_2O_5 NWs is as follows: ABTS and V_2O_5 NWs formation of a vanadium peroxo complex intermediate. In this process, substrate ABTS is oxidized and generation of superoxide (O^{2-}) in the presence of H_2O_2. As H_2O_2 is a two-electron oxidant, another molecule of ABTS is required for the regeneration of the V_2O_5 NWs resulting in the formation of an oxidative product (oxABTS).

Other metal oxide-based nanomaterials, such as MnO_2 (nanosheets, nanowires), NiO NPs, CeO_2 nanorods, and VO_2 (nanofibers, nanosheets, nanorods), are also proved to possess intrinsic peroxidase's activity. A suitable surface modification and metal doping to improve high affinity toward the substrates and catalytic activities of metal oxide nanomaterials were studied in many groups.[87–89,92,100,101]

2.4. Metal Nanomaterials

Metal-based nanomaterials including gold nanoparticles (nanoclusters) (Au NPs, Au NCs),[103–111] silver nanoparticles (Ag NPs),[112,113] platinum nanotubes (nanoclusters, nanoparticles) (Pt NTs, Pt NCs, Pt NPs),[114–117] rhodium nanoparticles (Rh NPs),[118] copper nanoparticles (nanoclusters) (Cu NPs, Cu NCs),[119,120] bimetal nanomaterials,[121–129] and iridium nanoparticles (Ir NPs),[130] were shown to have great intrinsic peroxidase-like activity and applied to various applications. The peroxidase-like activity of Au NPs was reported by Li et al. in 2010 for the first time.[104] They found that the positively charged Au NPs ((+) Au NPs) could catalyze the oxidation of substrate TMB in the presence of H_2O_2 to generate a blue color. A further systematic study of the origin of peroxidase-like activity of Au NPs was reported by Chen and co-workers.[109] They found that the peroxidase activity was indeed attributed to the Au NPs. Furthermore, the authors examined the effects of surface modification, and the results revealed that the activities could be adjusted by transforming the affinities between the

nanoparticles and substrates. Similarly, Ag NPs were also found to possess peroxidase-like activity in many groups.[112,113] Next, Cu NCs found to mimic peroxidase was reported by Xu et al. in 2013.[120] They found that the Cu NCs could catalyze the oxidation of substrate TMB in the presence of H_2O_2 to generate a blue color and the Cu NCs had a comparable affinity to TMB compared to HPR.

Ma and his groups proved Pt NCs possess peroxidase-like activity in 2011.[115] Subsequently, Pt NPs and Pt NTs were also reported to possess peroxidase-like activity.[114,116,117] Like the metal doping, alloying methods can improve the peroxidase catalytic activity as well. Bimetallic nanomaterials consist of two metals and often display enhanced catalytic performance than their monometallic counterparts because of a synergistic effect. Therefore, the peroxidase-like activity of bimetal nanomaterials such as Au@M (M = Ag, Pt, Bi, Cu),[121,124,126–129] AgM (M = Au, Pd, Pt),[122,125] and Fe–Co NPs[123] are studied by some groups. The mechanism of peroxidase-like activity of these metal nanomaterials is that metal nanomaterials can break up the O—O bond of H_2O_2 into two $\cdot$OH radical.

More recently, Ir NPs were found to possess peroxidase-like activity by Cui et al. in 2017.[130] Different from most metal nanomaterials, the peroxidase-like activity of Ir NPs is not dependent on the generation of $\cdot$OH radical. The authors confirmed that Ir NPs could promote the electron transfer between H_2O_2 and substrate TMB. The surface of Ir NPs absorb TMB and accept amino groups donated lone-pair electrons which leading to the increase of electron density of the Ir NPs. Then the electrons transfer from the Ir NPs to H_2O_2 and promote the oxidation of TMB.

2.5. Metal Sulfide Nanomaterials

The intrinsic peroxidase-like activity of metal sulfide-based nanomaterials including ZnS nanoparticles (ZnS NPs),[131] MoS_2 nanoparticles, nanoflakes, and nanosheets (MoS_2 NPs, MoS_2 NFs, and MoS_2 NSs),[30,132–138] nanostructured FeS,[139] CuS nanoparticles (CuS NPs),[140] VS_2 nanosheets (VS_2 NSs),[141] and WS_2 nanosheets (WS_2 NSs),[142] are widely explored and applied to various applications. Molybdenum disulfide (MoS_2), as one of the typical 2D layered transition metal dichalcogenides (2D-TMDs), has been widely used in many applications including biosensor, catalysis, and electronic devices due to its electronic properties and unique structure. Recently, the peroxidase-like activity of nanosize MoS_2 has drawn increasing research interest since it was reported by Guo et al. in 2014 for the first time.[134] The MoS_2 NSs can catalyze the reaction of peroxidase substrate OPD, ABTS, and TMB by H_2O_2 to generate color reaction, respectively. The MoS_2 NSs display a high catalytic activity with a wide pH range (2.0–7.5), which is wider than that of other peroxidase-like nanomaterials, such as Fe_3O_4 NPs,[32] Co_3O_4,[93] $ZnFe_2O_4$ NPs,[48] TiO_2 nanotubes,[143] Pt nanotubes,[117] Fe–Co bimetallic alloy NPs,[123] SWCNTs[62] carbon nitride dots,[72] carbon nanodots,[68] and GO.[65] They confirmed that the catalytic mechanism of MoS_2 NSs was attributed to the production of $\cdot$OH by decomposing H_2O_2. The TMB molecules were absorbed on the surfaces of MoS_2 NSs and donated

**ADVANCED
SCIENCE NEWS**
www.advancedsciencenews.com

NANO · MICRO
small
www.small-journal.com

lone-pair electrons from the amino groups to MoS_2 NSs, which induced a raising of electron mobility and density in the MoS_2 NSs therefore to accelerate the reaction rate of TMB oxidation by ·OH. Following this creatively discovery, different shapes of nanosize MoS_2, surface modification as well as preparation methods to improve catalytic property were reported by many groups.[30,133,135–138]

Other metal sulfide nanomaterials such as ZnS NPs,[131] nanostructured FeS,[139] CuS NPs,[140] and WS_2 NSs[142] are proved to possess intrinsic peroxidase's activity as well. The peroxidase-like catalytic mechanism of those metal sulfide nanomaterials are attributed to the generation of ·OH by decomposing H_2O_2.

2.6. Nanocomposites

Hybrid composite nanomaterials (nanocomposites), show well-defined structures, have been widely explored to realize cooperatively enhanced properties or to achieve the combination of the respective characteristics of each component. Nanocomposites usually show enhanced intrinsic properties of each ingredient or bring novel functions and properties or promoted dispersibility and stability. Therefore, the peroxidase-like of nanocomposites was studied by many researchers. Fan et al.[144] reported that the nanocomposites (MWCNTs/Fe_3O_4 MNPs) possess peroxidase-like catalytic activity for the first time in 2009. The as-prepared MWCNTs/Fe_3O_4 MNPs nanocomposites retained the magnetic properties of individual Fe_3O_4 MNPs which can be effectively separated under an external magnetic field. More importantly, the formation of the MWCNTs/Fe_3O_4 MNPs nanocomposites enhanced the intrinsic peroxidase-like activity of the Fe_3O_4 MNPs. The enhanced peroxidase-like activity can be caused by the synergetic effect of MWCNTs and Fe_3O_4 MNPs. Fe_3O_4 MNPs as catalyzing elements, MWCNTs as substrate absorbing species, showed high affinity for substrates due to its high surface-to-volume ratios. Other enhanced peroxidase-like activity of MNPs-based nanocomposites such as carbon-coated MNPs (Fe_3O_4@C[145]), GO–Fe_3O_4 MNPs,[146] magnetic mesoporous silica nanoparticles (Fe_3O_4@MSN[147]), Fe_3O_4@SiO_2@Au MNPs,[148] and g-C_3N_4–Fe_3O_4 MNPs,[149] are also studied by researchers.

Fan et al.[150] reported that Au–Pd bimetallic nanoparticles anchored MoS_2 nanosheets (Au–Pd/MoS_2) possessed peroxidase-like activity. Compared with pure MoS_2 nanosheets, the Au–Pd/MoS_2 hybrid exhibits high catalytic activity. The enhanced peroxidase-like activity of Au–Pd/MoS_2 hybrid is not only due to the intrinsic catalytic activity of MoS_2 nanosheets, but also due to the strong interaction of metal–support and metal–metal. Au–Pd NPs increase the surface charge heterogeneity, improving the affinity toward substrates. Meanwhile, the metal–support interaction can also promote the electron transfer from Au–Pd NPs to the MoS_2 nanosheets which reduce the activation energy. Similarly, the enhanced peroxidase-like activity of Pt–Ag bimetallic nanoparticles decorated MoS_2 nanosheets (Pt–Ag/MoS_2) hybrid was reported by Yang et al.[151] More recently, Weng et al.[152] reported the enhanced peroxidase-like activity of graphene oxide and MoS_2 (GO/MoS_2) hybrid. Replacing noble bimetallics with GO can

decrease the cost of noble metals, which can expand its further application. The excellent peroxidase-like activity of GO/MoS_2 hybrid is attributed to the enhanced electron transfer on the surface of GO/MoS_2 and the synergistic interaction of two components.

Except for above-mentioned nanocomposites, other novel nanocomposites are also designed to possess enhanced peroxidase-like activity. Those nanocomposites including TiO_2@CeO_x core–shell nanoparticles,[153] MnSe loaded g-C_3N_4 nanocomposite,[154] Au@Ag–hemin modified reduced graphene oxide sheets,[155] Cu–Ag bimetallic nanoparticles decorated reduced graphene oxide sheets,[156] graphene supported Au–Pd bimetallic nanoparticles,[157] graphene quantum dots–copper oxide nanocomposites (GQDs/CuO),[158] TiO_2-encapsulated Au (Au@TiO_2) yolk–shell nanostructure,[159] $CoSe_2$/reduced graphene oxide ($CoSe_2$/rGO) hybrid,[160] and montmorillonite-supported ZnS,[161] and CuS[140] and Ag_2S[162] nanocomposites. The enhanced peroxidase-like activity of those nanocomposites are attributed to synergistic interaction of two components as well.

3. Glucose Biosensor

3.1. Magnetic Nanomaterial-Based Glucose Biosensor

The first application of peroxidase-like activity of Fe_3O_4 MNPs for colorimetric detection of glucose was reported by Wang and co-workers in 2008.[37] This work was based on the novel performance of Fe_3O_4 MNPs as peroxidase mimetics which was first developed by Yan et al. in 2007. In Wang's work, Fe_3O_4 MNPs were able to catalyze the oxidation of a peroxidase substrate ABTS in the presence of H_2O_2 to the oxidized colored product, which provided colorimetric detection of H_2O_2. They combined the Fe_3O_4 MNPs catalytic reaction and the catalytic reaction of glucose with GOx, and developed a colorimetric biosensor for glucose detection. The developed biosensor showed sensitive and selective response to glucose detection. The developed analytical method showed sensitive detection of glucose with a linear range from 5×10^{-5} to 1×10^{-3} mol L^{-1} and a detection limit of 3×10^{-5} mol L^{-1}. The selectivity of this developed method showed high selectivity toward glucose over maltose, lactose, and fructose.

Bare Fe_3O_4 MNPs often show aqueous instability and much weaker affinity toward substrates than HPR, which leads to low catalytic activities and restricts its applications. A suitable surface modification may solve those problems. The first research of surface functionalization of peroxidase-like activity of Fe_3O_4 MNPs and its application for colorimetric detection of glucose was reported by Yu and co-workers in 2009.[163] In this work, authors explored the peroxidase-like activity of Fe_3O_4 MNPs and found that the peroxidase-like activity relied on the surface properties (charge intensity, surface charge, and coating thickness) of nanoparticles. The authors prepared seven kinds of Fe_3O_4 MNPs including unmodified Fe_3O_4 MNPs (M_{nat}), citrate- and glycine-modified Fe_3O_4 MNPs (M_{cit}, M_{gly}), polylysine- and poly(ethyleneimine)-coated Fe_3O_4 MNPs (M_{PLL}, M_{PEI}), and carboxymethyl dextran- and heparin-coated Fe_3O_4 MNPs (M_{CMD}, M_{hep}). Surprisingly, the result showed that

anionic nanoparticles exhibited a high catalytic activity and had a high affinity with TMB as a substrate. The activity gradually increased when changing the zeta potential from positive to negative. M_{hep} showed a 5.9-fold higher catalytic activity than M_{PEI}. With ABTS as the substrate, anion nanoparticles exhibited a low affinity and subsequently a low peroxidase activity. The activity decreased dramatically in changing the zeta potential from positive to negative. M_{PEI} exhibited an 11.5-fold higher activity than M_{hep}. Those discoveries can be attributed to TMB possess two amine groups, likely exhibiting stronger affinity toward a negatively charged nanoparticle surface. Conversely, ABTS carries two sulfonic acid groups, likely yielding higher affinity toward a positively charged nanoparticle surface. Finally, the authors used M_{gly} and M_{hep} to detect glucose. The detection limit of M_{gly} and M_{hep} was calculated to be 8.5×10^{-6} mol L^{-1} and 1.58×10^{-5} mol L^{-1}, respectively.

In a follow-up project, Yu and co-workers[164] further discovered that substrate-specific surface modification could effectively improve the particle' affinity toward substrates such as ABTS or TMB therefore to enhanced the interaction with ABTS or TMB, respectively. The authors prepared four kinds of superficially modified Fe_3O_4 MNPs including aminated Fe_3O_4 MNPs (NH_2–Fe_3O_4 MNPs), thiolated Fe_3O_4 MNPs (SH–Fe_3O_4 MNPs), thiolated and aminated Fe_3O_4 MNPs (SH–NH_2–Fe_3O_4 MNPs), and citrated-coated Fe_3O_4 MNPs (cit-Fe_3O_4 MNPs). The result displayed that the affinity toward TMB prompted by introducing of sulfhydryl groups, because of the specific interaction of TMB with SH groups. Similarly, the affinity toward ABTS enhanced by incorporating of amine groups which shows a strong electrostatic attraction of substrate ABTS with amine groups. Owing to its features of both amine and sulfhydryl groups, SH–NH_2–Fe_3O_4 MNPs displayed a much lower K_m, ABTS value and K_m, TMB value, or dual improved affinity toward both ABTS and TMB, and good particle stability. As a result, among the tested particles SH–NH_2–Fe_3O_4 MNPs exhibited the lowest LOD and highest sensitivity in glucose detection. The SH–NH_2–Fe_3O_4 MNPs exhibited sensitive detection of glucose with a linear range from 1.2×10^{-7} mol L^{-1} to 4×10^{-6} mol L^{-1} and a detection limit of 5×10^{-7} mol L^{-1}, which was lower than that of bare Fe_3O_4 MNPs (3×10^{-5} mol L^{-1}). Those developed researches can be the breakthrough for the improvement of catalytic ability and for eventual enhancement of the sensitivity and detection limit in glucose detection and provide a theoretical basis for further studies.

Based on those studies, many other novel and creative surface modification of Fe_3O_4 MNPs were developed for colorimetric detection of glucose. For examples, Yu et al.[56] developed a poly(diallyldimethylammonium chloride)-coated Fe_3O_4 MNPs (PDDA–Fe_3O_4 MNPs) for colorimetric sensing of glucose. The cationic-containing PDDA showed stronger affinity toward ABTS. The linear range of this colorimetric biosensor was in the range of 3.0×10^{-5} to 1.0×10^{-4} mol L^{-1} and 2.0×10^{-4} to 1×10^{-3} mol L^{-1}, and the limit of detection (LOD) was as low as 3.0×10^{-5} mol L^{-1}. More recently, Liu and co-workers developed an efficient colorimetric glucose biosensor based on peroxidase-like of protein–Fe_3O_4 MNPs.[59] The peroxidase-like of casein–Fe_3O_4 MNPs exhibited good dispersibility, stability, and catalytic performance compared with bare MNPs. Fe_3O_4 MNPs modified with casein significantly improved the affinity toward

both TMB and H_2O_2. This method was low-cost and simple, and showed highly selective and sensitive for glucose detection with a LOD of 1.0×10^{-6} mol L^{-1} over a linear range from 3.0×10^{-6} mol L^{-1} to 1.0×10^{-3} mol L^{-1}. Other materials such as ATP[55] and porphyrin[60] were also used to modify Fe_3O_4 MNPs to enhance the peroxidase catalytic activities and improve the detection limit and sensitivity in glucose detection (see **Table 1**).

Except for surface modification, metal doping was also studied to improve the peroxidase-like catalytic activity of Fe_3O_4 MNPs and applied to detect glucose. Hosseini et al. reported the cerium-doped Fe_3O_4 MNPs (Ce–Fe_3O_4 MNPs) with enhanced peroxidase-like catalytic activity for colorimetric biosensing of glucose.[57] The peroxidase-like activity of Ce–Fe_3O_4 MNPs was tested by catalyzing the reaction of peroxidase substrate TMB to produce a color reaction in the presence of H_2O_2. The result showed that the peroxidase-like activity of Ce–Fe_3O_4 MNPs dramatically improved with the Ce doping. Moreover, kinetic assay indicated that the Ce–Fe_3O_4 MNPs possessed higher affinity to H_2O_2 compared to HPR and bare Fe_3O_4 MNPs. The enhanced peroxidase-like activity of Ce–Fe_3O_4 MNPs was attributed to the synergetic interaction between Fe^{2+} and Ce^{3+}. Finally, Ce–Fe_3O_4 MNPs were used for colorimetric detection of glucose. The developed biosensor with a linear range from 5×10^{-6} to 1.5×10^{-4} mol L^{-1} and a detection limit of 1.2×10^{-6} mol L^{-1}, which was lower than that of bare Fe_3O_4 MNPs (3×10^{-5} mol L^{-1}).

Another way to avoid intrinsic instability of bare Fe_3O_4 MNPs for enhancement of the sensitivity and detection limit in glucose detection is to look for more stable peroxidase-like of MNPs. The cubic spinel structured MFe_2O_4 MNPs are an important kind of iron oxide magnetic materials, in which oxygen forms a face-centered cubic (fcc) close packing. The octahedral interstitial sites are occupied by M^{2+} and half of Fe^{3+} ions, while the tetrahedral sites are occupied by the other half Fe^{3+} ions. MFe_2O_4 MNPs compounds was synthesized by using divalent metal ions instead of Fe^{2+} ions Fe_3O_4, which showed a good resistance to the oxidation of Fe^{2+} in air atmosphere. MFe_2O_4 MNPs show notably properties such as large surface area to volume ratio, high saturation magnetization, nanometer size, and superparamagnetic behavior. The peroxidase-like of MFe_2O_4 MNPs was first reported by Shi et al. in 2011.[50] They found that the $CoFe_2O_4$ MNPs showed significant peroxidase activity and developed a new chemiluminescent method for glucose detection. The LOD of this chemiluminescent method was as low as 2.4×10^{-8} mol L^{-1}. Later, the peroxidase-like of $ZnFe_2O_4$ MNPs was reported by Su and co-workers in 2012.[48] The $ZnFe_2O_4$ MNPs exhibited several advantages such as rapid separation, good stability, high catalytic efficiency, and monodispersion over HRP and other peroxidase nanomaterials. Results revealed that the peroxidase-like catalytic activity was 5.0×10^5 and 1.0×10^7 times higher than that of Fe_3O_4 MNPs and HRP, respectively. Finally, $ZnFe_2O_4$ MNPs were used as a colorimetric glucose biosensor. This biosensor is highly selective and sensitive, low-cost, and simple for glucose detection by using GOx and with a detection limit of 3.0×10^{-7} mol L^{-1} and the linear range from 1.25×10^{-6} mol L^{-1} to 1.875×10^{-5} mol L^{-1}. More recently, MFe_2O_4 (M = Mg, Ni, Cu) MNPs were also found to possess peroxidase activity by the same groups.[45] Meanwhile, they revealed that the MFe_2O_4 (M = Ni, Mg, Cu) MNPs also with catalase-like activity. Such dual enzyme-like

Table 1. Glucose detection with peroxidase-like of magnetic nanomaterials.

Magnetic nanomaterials	Features of catalytic reactions	Comments	Optimum pH	Linear range [µM]	LOD [µM]	Reference
Fe_3O_4 MNPs	Fenton's reagent (i.e., Fe^{2+}/Fe^{3+} ions) catalyze the H_2O_2 generate •OH	Substrate: ABTS; Selectivity against sugars: fructose, lactose, and maltose	3.5	50–1000	30	[37]
Casein–Fe_3O_4 MNPs	Casein improve the affinity to TMB and H_2O_2	Substrate: TMB Selectivity against sugars: fructose, lactose, and maltose	4.0	3–1000	1	[59]
ATP mediated Fe_3O_4 MNPs	ATP mediate Fe_3O_4 MNPs catalytic at neutral pH	Substrate: TMB; Glucose in human blood samples was tested	7.4	50–4000	50	[55]
Magnetic hydrogels prepared Fe_3O_4 MNPs	—	Substrate: TMB; Selectivity against sugars: fructose, lactose, and maltose	4.0	1–40	0.37	[179]
Poly(diallyldimethylammonium chloride)-coated Fe_3O_4 MNPs	PDDA-coated Fe_3O_4 MNPs with positive charge show high affinity for ABTS	Substrate: ABTS; Glucose in serum samples was tested; Selectivity against sugars: galactose, lactose, mannose, maltose, arabinose, cellobiose, raffinose, and xylose	2.0	30–100 200–1000	30	[56]
Magnetic iron oxide nanoparticles	Iron oxide NPs coated with glycine show high affinity to ABTS	Substrate: ABTS; Iron oxide NPs were coated with glycine; More robust than HRP toward NaN_3 inhibition	—	31.2–250	8.5	[163]
	Iron oxide NPs coated with heparin show high affinity to TMB	Substrate: ABTS; Iron oxide NPs were coated with heparin; More robust than HRP toward NaN_3 inhibition	—	31.2–250	15.8	
Ce-doped Fe_3O_4 MNPs	Ce^{3+} and Fe^{2+} as Fenton's reagent to generate the •OH; Ce^{3+}/Ce^{4+} cycling facilitates electron transfer between H_2O_2 and TMB	Substrate: TMB; Glucose in serum samples was tested; Selectivity against sugars: maltose, fructose, sucrose, uric acid, ascorbic acid	3.0	5–150	1.5	[57]
Porphyrin modified Fe_3O_4 MNPs	Fe^{3+} catalyze the H_2O_2 generate •OH; Porphyrin enhance the catalytic activity by photoinduced electron–hole pairs	Substrate: TMB; Glucose in serum samples was tested; Selectivity against sugars: maltose, fructose, sucrose, lactose	3.8	5–25	2.21	[60]
Magnetic iron oxide nanoparticles	$-SH-NH_2$-coated iron oxide NPs show highest high affinity for both ABTS and H_2O_2	Substrate: ABTS; Iron oxide NPs were coated with citrate, $-NH_2$, $-SH$, $-SH-NH_2$	4.0	0.12–4	0.5	[164]
$CoFe_2O_4$ MNPs	Co^{2+} and Fe^{3+} as Fenton's reagent to generate the •OH	Substrate: TMB; Chemiluminescence detection of glucose	6.0	0.1–10	0.024	[50]
Chitosan modified $CoFe_2O_4$ MNPs	Chemiluminescence detection of glucose	Substrate: TMB; Glucose in serum samples was tested	—	0.05–10	0.52	[47]
$ZnFe_2O_4$ MNPs	Fe^{3+} catalyze the H_2O_2 generate •OH	Substrate: TMB; Glucose in urine samples was tested; Selectivity against sugars: fructose, lactose, and maltose	4.5	1.25–18.75	0.3	[48]
MFe_2O_4 (M = Mg, Ni, Cu) MNPs	Fe^{3+} catalyze the H_2O_2 generate •OH; MFe_2O_4 (M = Mg, Ni, Cu) MNPs also can catalyze H_2O_2 generate O_2	Substrate: ABTS; $NiFe_2O_4$ MNPs was used for detect glucose; Selectivity against sugars: fructose, lactose, and maltose	4.0	0.94–25	0.45	[45]
Fe_3S_4 MNPs	—	Substrate: TMB; Glucose in serum samples was tested; Selectivity against sugars: maltose, fructose, sucrose, lactose, galactose	6.78	2–100	0.16	[54]

ADVANCED
SCIENCE NEWS

www.advancedsciencenews.com

NANO · MICRO
small
www.small-journal.com

catalytic activities of MFe_2O_4 (M = Ni, Mg, Cu) MNPs were first discovered. $NiFe_2O_4$ MNPs were used as a colorimetric glucose biosensor with a detection limit of 4.5×10^{-7} mol L^{-1} and the linear range from 9.4×10^{-7} mol L^{-1} to 2.5×10^{-5} mol L^{-1} under the optimum conditions,. The colorimetric glucose biosensor based on peroxidase-like of magnetic nanomaterial are summarized in Table 1.

3.2. Carbon Nanomaterial-Based Glucose Biosensor

The intrinsic peroxidase-like activity of carbon nanomaterials (SWCNTs) was first reported by Song et al. in 2009.[62] But the first application of peroxidase-like activity of carbon nanomaterials (GO) for colorimetric detection of glucose was reported by Song et al. in 2010.[65] Their research results revealed that GO–COOH showed intrinsic peroxidase-like activity and its catalysis was strongly influence by H_2O_2 concentration, temperature, and pH, similar to HPR. GO–COOH could induced the peroxidase substrate TMB to generate a blue color reaction in the presence of H_2O_2. Kinetic analysis showed that the catalysis with a ping-pong mechanism. Compared with HRP, the GO–COOH had a higher catalytic activity to TMB. Compared to natural enzymes, GO–COOH possesses several advantages, such as stability, inexpensive, and ease of preparation. Moreover, GO–COOH had high affinity to organic substrates through hydrophobic and π–π interactions as well as high surface-to-volume ratios compared to Fe_3O_4 MNPs and HRP. According to this finding, the authors designed a highly sensitive and selective, low-cost, simple colorimetric biosensor to detect glucose with a linear range of 1.0×10^{-6} to 2.0×10^{-5} mol L^{-1} and a detection limit of 1.0×10^{-6} mol L^{-1}. Moreover, this developed method can detect glucose in fruit juice and diluted blood samples or buffer solution.

In recent years, fullerene (C_{60}) has garnered intensive interest due to its excellent electron acceptor capability in nanomaterials biotechnology and science. Fullerene (C_{60}) can accept as many as six electrons reversibly.[165] However, the application of peroxidase-like activity of C_{60}-carboxyfullerene ($C_{60}[C(COOH)_2]_2$) for the colorimetric biosensing of glucose was reported by Li and co-workers.[66] The result displayed that $C_{60}[C(COOH)_2]_2$ could catalyze the reaction of peroxidase substrate TMB to generate a blue color reaction in the presence of H_2O_2. Kinetic studies further displayed that $C_{60}[C(COOH)_2]_2$ possessed an even high affinity to TMB compared to the natural enzyme, HRP. In addition, $C_{60}[C(COOH)_2]_3$ and $C_{60}[C(COOH)_2]_4$ were also studied and found to possess peroxidase catalytic activity. $C_{60}[C(COOH)_2]_2$ showed highest catalytic activity toward H_2O_2 and TMB under the same condition. This difference should be attributed to the synergistic effects from conjugated degree and size distributions of fullerene cage. Finally, the $C_{60}[C(COOH)_2]_2$/GOx/TMB system provided a novel colorimetric biosensor for glucose and showed good response with a LOD of 5.0×10^{-7} mol L^{-1} and over a range of 1.0×10^{-6} to 4.0×10^{-5} mol L^{-1}.

The intrinsic peroxidase-like activity of g-C_3N_4 was reported by Lin et al.[74] and Tian et al.[73] In Liu's study,[74] they found that the g-C_3N_4 could caused the obvious oxidation of TMB in the condition of visible light even in the absence of H_2O_2. This can be attributed to the excellent photocatalytic property

of g-C_3N_4. Therefore, the study of peroxidase-like activity of g-C_3N_4 was tested in dark. The result revealed that the g-C_3N_4 could catalyze the oxidation of TMB in the presence of H_2O_2 to generate the typical blue color reaction and the catalytic activity was strongly influenced by temperature, pH, and the concentration of catalyst and H_2O_2. Based on the peroxidase-like activity of g-C_3N_4, the authors developed a colorimetric biosensor for the detection of glucose. The linear range for glucose was from 5.0×10^{-6} to 1.0×10^{-4} mol L^{-1} and the LOD was 1.0×10^{-6} mol L^{-1}. Similarly, Tian et al.[73] found that the ultrathin g-C_3N_4 nanosheets possessed peroxidase-like activity. Furthermore, they demonstrated that the Fe-doped g-C_3N_4 nanosheets (Fe–g-C_3N_4) led to peroxidase activity of g-C_3N_4 with greatly enhanced catalytic performance (**Figure 4**). Results showed that the g-C_3N_4 and Fe–g-C_3N_4 both had higher affinity for TMB than HPR. Fe doping-mediated catalytic property improvement of g-C_3N_4 nanosheets can be illustrated as follows. g-C_3N_4 is a visible-light photocatalyst which can translate Fe^{3+} into Fe^{2+}. Fe^{2+}-H_2O_2 is a well-known Fenton's reagent with excellent property catalyzing the oxidation of organic substrates. Fe^{2+} catalyze the oxidation of the TMB in the presence of H_2O_2 and itself convert to Fe^{3+} at the same time in the reaction. Simultaneously, the newly formed Fe^{3+} from Fe^{2+} oxidized by H_2O_2 is immediately convert back to Fe^{2+} through receiving electrons from g-C_3N_4. This catalytic cycle could be repeated rapidly until the consumption of TMB or H_2O_2. On the other hand, the rapid electron transfer from the conduction band of g-C_3N_4 to Fe^{3+} result in more effective charge separation in g-C_3N_4, which facilitated electron transfer from TMB to g-C_3N_4 and thus accelerate the oxidation of TMB (Figure 4). Based on the peroxidase-like activity of Fe–g-C_3N_4, the authors developed a colorimetric biosensor for the detection of glucose. The linear range for glucose was from 5.0×10^{-7} to 1.0×10^{-5} mol L^{-1} and the LOD was as low as 5.0×10^{-7} mol L^{-1} which was lower than that of bare g-C_3N_4 (1.0×10^{-6} mol L^{-1}).

Carbon dots (CDs), a new class of the carbon nanomaterials family, has received much attention because of its excellent fluorescence properties, such as high photo stability against photo blinking and bleaching and excitation-dependent emission. Furthermore, CDs are small in size, low in toxicity and
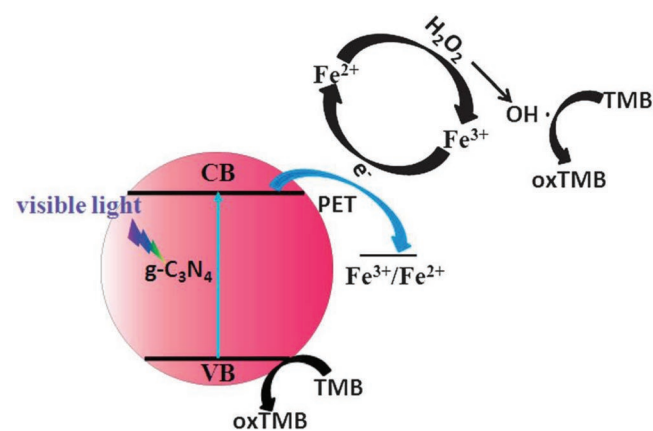

Figure 4. A schematic illustration of the Fe doping-mediated catalytic performance enhancement of g-C_3N_4 nanosheets. Reproduced with permission.[73] Copyright 2013, The Royal Society of Chemistry.

molecular weight, and good biocompatible. These unique performances make the CDs excellent potential substitutes for organic dyes and semiconductor quantum dots in bioimaging and biolabeling. The peroxidase-like activity of CDs and application for colorimetric biosensing of glucose was first reported in 2011.[68] Peroxidase substrates including OPD and TMB were used to evaluate the peroxidase-like activity of CDs. In the presence of H_2O_2, CDs can catalyze the oxidation of two substrates. Results showed that the CDs had high affinity to TMB than HPR due to the relatively small K_m values. Based on the peroxidase-like activity of CDs, the authors developed a colorimetric biosensor for the detection of glucose. The linear range for glucose was from 1.0×10^{-6} mol L^{-1} to 5.0×10^{-5} mol L^{-1} and the LOD was as low as 4.0×10^{-7} mol L^{-1}. Later, intrinsic peroxidase-like activity of the reduced state carbon dots (r-CDs) was found by Long and co-workers.[67] r-CDs can catalyze the oxidation of TMB to generate a color reaction in the presence of H_2O_2 as well. In the works, they compared the catalytic activity of r-CDs and CDs and discovered that the catalytic activity of r-CDs was lower than that of CDs. The reasons are the surfaces of r-CDs contains COOH and −OH groups, and the surfaces of CDs contains −COOH, −C=O groups. According to previous reports,[77] −COOH groups are the substrate-binding sites, −C=O groups act as catalytically active sites, while −OH groups can even restrain the catalytic reaction. Therefore, the catalytic activity of CDs was higher than that of r-CDs. Based on the peroxidase-like activity of r-CDs, the authors developed a colorimetric biosensor for the detection of glucose. The linear range for glucose was from 1.0×10^{-5} to 4.0×10^{-5} mol L^{-1} and the LOD was 2.0×10^{-6} mol L^{-1} which was lower than that of CDs. More recently, Wang et al.[69] synthesized a novel catalytically active CDs by simply hydrothermal method using animal blood as carbon source. These prepared novel CDs were found to contain nitrogen, oxygen, carbon elements and trace amount of iron and sulfur species. The multielement-doped carbon dots (ME-CDs) reveal excellent peroxidase-like catalytic activities which are attributed to the doped trace amount of iron elements. The authors used the peroxidase-like of ME-CDs to manufacture a colorimetric glucose biosensor. The linear range for glucose was from 2.0×10^{-4} mol L^{-1} to 2.5×10^{-3} mol L^{-1} and the LOD was 6.0×10^{-5} mol L^{-1}.

Other carbon nanomaterials such as carbon nitride dots,[72] nitrogen-doped graphene quantum dots (N-GQDs),[75] boron-doped carbon quantum dots (B-CQDs),[71] graphene dots (GDs)[76] were confirmed to possess intrinsic peroxidase-like activity and used to fabricate colorimetric glucose biosensor as well (see in **Table 2**). Those peroxidase-like of carbon-based nanomaterials were showed a good selectivity and sensitivity for the detection of glucose.

3.3. Metal Oxide Nanomaterial-Based Glucose Biosensor

The intrinsic peroxidase-like activity of CuO NPs was first reported by Chen et al.[84] However, the easy sedimentation and aggregation of the commercial CuO NPs affect their further applications in aqueous systems to some extent. Therefore, the Chen's group fabricated the water-soluble CuO NPs for the biosensing of glucose.[81] Peroxidase substrates such as DAB, ABTS,

and TMB were used to assess the peroxidase-like activity of the water-soluble CuO NPs. In the presence of H_2O_2, the water-soluble CuO NPs can catalyze the oxidation of three substrates by generation of ·OH radicals. Results indicated that the water-soluble CuO NPs had higher affinity toward TMB than HPR. Under the same conditions, the peroxidase-like catalytic activity of the water-soluble CuO NPs is about 100 times compared to commercial CuO NPs. The reason of the peroxidase-like catalytic activity can be caused by Cu^{2+} leaching from CuO NPs in the solutions. Based on the peroxidase-like activity of water-soluble CuO NPs, the authors developed a colorimetric biosensor for the detection of glucose. The linear range for glucose was from 1.0×10^{-4} mol L^{-1} to 8.0×10^{-3} mol L^{-1}. More recently, the same groups developed a fluorescent glucose biosensor based on the peroxidase-like activity of CuO NPs.[82] This designed fluorescent glucose biosensor had a linear range of 3.0×10^{-6} to 1.0×10^{-3} mol L^{-1} and with a LOD of 1.0×10^{-6} mol L^{-1}. Metal doping for enhanced peroxidase-like activity of CuO NPs was also studied by researcher. In Gedanken's works,[83] they reported the Zn-doped CuO NPs (Zn-CuO NPs) with enhanced peroxidase-like activity and applied to colorimetric glucose biosensor. Results showed that the Zn-CuO NPs had higher affinity for H_2O_2 and TMB than CuO and HPR. In addition, ·OH radicals capture assay revealed that the Zn-CuO NPs generated more ·OH compared with CuO or ZnO. The unorganized lattice of Zn-CuO can be contributed to this enhancement. The introduction of high energy of the acoustic cavitation into the product in sonochemically synthesized metal oxides resulting in a disorganized and perturbed Zn-CuO lattice rich in vacancies, dislocations, and defects, which are active sites for the formation of ·OH radicals. Finally, Zn-CuO NPs were used as a colorimetric biosensor for the determination of glucose. The developed method with a linear range from 2.5×10^{-5} to 5×10^{-4} mol L^{-1} and a detection limit of 1.5×10^{-6} mol L^{-1}, which was lower than that of undoped CuO NPs (1×10^{-4} mol L^{-1}).

The peroxidase-like activity of Co_3O_4 NPs and its application for colorimetric detection of glucose was first reported by Wang et al. in 2012.[93] As described in Section 2.3, the Co_3O_4 NPs had a high affinity for TMB compare to HPR. This could be ascribed to the surface of the Co_3O_4 NPs contain more "active sites" compared with HPR. Based on the peroxidase-like activity of Co_3O_4 NPs, the authors developed a colorimetric biosensor for the detection of glucose. The linear range for glucose was from 1.0×10^{-5} to 1.0×10^{-2} mol L^{-1} and the LOD was 5.0×10^{-6} mol L^{-1}. The excellent peroxidase-like activity of Co_3O_4 NPs was further proved in a subsequent study.[90] In this study, the authors not only developed a colorimetric biosensor for the determination of glucose based on the peroxidase-like activity of Co_3O_4 NPs, but studied the inhibitory effects of nature antioxidants on peroxidase mimics by using the peroxidase-like activity of Co_3O_4 NPs. Three natural antioxidants, ascorbic acid (AA), tannic acid (TA), and gallic acid (GA), were used to compare antioxidant abilities. They discovered that these three antioxidants efficiently inhibited peroxidase-like activity with concentration-dependence. The antioxidants displayed different efficiencies, in the following order: TA > GA > AA. This study act as a proof-of-concept that nanoenzyme mimics can be used to screen enzyme inhibitors and to assess antioxidant abilities. The designed colorimetric glucose biosensor in this work

Table 2. Glucose detection with peroxidase-like of carbon nanomaterials.

Carbon nanomaterials	Features of catalytic reactions	Comments	Optimum pH	Linear range [µM]	LOD [µM]	Reference
Carboxyl-modified graphene oxide	Electron transfer between graphene and H_2O_2 induce the catalytic reaction	Substrate: TMB; Selectivity against sugars: fructose, lactose, and maltose	4.0	1–20	1	[65]
C_{60}-carboxyfullerene	TMB is absorbed on the surface of carbon cages by π–π stacking interaction; Electron transfer from carbon cage to H_2O_2 induce the catalytic reaction	Substrate: TMB; Glucose in serum samples was tested; Selectivity against sugars: fructose, sucrose	3.5	1–40	0.5	[66]
Carbon nitride dots	—	Substrate: TMB	3.0	1–5	0.5	[72]
Fe-doped g-C_3N_4	Fe enhance the catalytic activity of g-C_3N_4 by the Fe^{2+}; g-C_3N_4 absorb the TMB	Substrate: TMB; Selectivity against sugars: fructose, lactose, and maltose	4.0	0.5–10	0.5	[73]
g-C_3N_4	Photocatalytic reaction for the reaction was conducted in dark	Substrate: TMB; Glucose in serum samples was tested	3.0	5–100	1	[74]
Nitrogen-doped graphene quantum dots	The electron transfers from the N-GQDs to H_2O_2 induce the catalytic oxidation of TMB	Substrate: TMB; Selectivity against sugars: fructose, lactose, maltose, and sucrose	3.0	25–375	16	[75]
Multielement-doped carbon dots	Carboxylic groups (O=C—O—) as substrate binding sites	Substrate: TMB; Selectivity against sugars: fructose, lactose, maltose, and sucrose	4.5	200–2500	60	[69]
Carbon nanodots	C-Dots induce the •OH production by catalyzing the decomposition of H_2O_2	Substrate: TMB; Glucose in serum samples was tested; Selectivity against sugars: fructose, lactose and maltose	3.5	1–50	0.4	[68]
Reduced state carbon dots	The catalytic activity of CDs is higher than that of r-CDs	Substrate: TMB; Glucose in serum samples was tested; Selectivity against sugars: fructose, lactose, and maltose	3.0	10–40	2	[67]
Boron-doped carbon quantum dots	The electron transfers from the BCQDs to H_2O_2 induce the catalytic oxidation of TMB	Substrate: TMB	7.4	8–80	8	[71]
Carbon nanodots	—	Substrate: TMB; Glucose in serum samples was tested; Selectivity against sugars: fructose, lactose, and maltose	4.4	20–600	5.2	[70]
Graphene dots	The GDs show higher catalytic activity than GO due to the small size	Substrate: TMB; Glucose in serum samples was tested; Selectivity against sugars: fructose, sucrose, galactose, and maltose	4.0	0.5–200	0.5	[76]

showed a linear range of 2.0×10^{-5} to 2.0×10^{-4} mol L^{-1} and with a LOD of 5.0×10^{-6} mol L^{-1}. An enhancement of peroxidase-like activity of porphyrin modified Co_3O_4 NPs (por-Co_3O_4 NPs) was reported by Liu and co-workers.[92] The catalytic oxidation of substrate TMB in the presence of H_2O_2 was used to evaluate the peroxidase-like activity of the por-Co_3O_4 NPs. Results showed that the por-Co_3O_4 NPs had a high affinity for TMB compared to bare Co_3O_4 NPs, HPR, and other reported nanomaterials such as Co_3O_4 NPs and Fe_3O_4 MNPs. More interestingly, the por-Co_3O_4 NPs were proved to show high peroxidase activity compared to bare Co_3O_4 NPs. Based on the peroxidase-like activity of por-Co_3O_4 NPs, the authors developed a colorimetric biosensor for the detection of glucose. The linear range for glucose was from 1.0×10^{-6} to 1.0×10^{-5} mol L^{-1} and the LOD was as low as 8.6×10^{-7} mol L^{-1}, which was lower than that of bare Co_3O_4 NPs.[90,93]

In recent years, cerium oxide has obtained great interest because of its unique chemical and physical performances.

The peroxidase-like activity of CeO_2 NPs and application for colorimetric detection of glucose was reported by Wang et al. in 2012 for the first time.[85] As described in Section 2.3, the CeO_2 NPs had high affinity for TMB compare to HPR. Based on the peroxidase-like activity of CeO_2 NPs, the authors fabricated a colorimetric biosensor for the biosensing of glucose. The linear range for glucose was from 6.6×10^{-6} to 1.3×10^{-4} mol L^{-1} and the LOD was 3×10^{-6} mol L^{-1}. A suitable surface modification to improve the peroxidase-like activity of cerium oxide and for improvement of the sensitivity and detection limit in glucose was reported in Liu's groups.[86,87] Porphyrin plays an important role in oxidative mechanisms of metabolism, ranging from the oxidative reactions of peroxidase enzymes and cytochrome to the oxygen-carrying ability of haemoglobins. Therefore, the authors used porphyrin both to modify CeO_2 NPs (por-CeO_2 NPs) and CeO_2 NRs (por-CeO_2 NRs) and study the peroxidase-like activity of por-CeO_2 NPs and por-CeO_2 NRs. The peroxidase-like activity of por-CeO_2 NPs and

por-CeO$_2$ NRs were assessed by the catalytic oxidation of substrate TMB in the presence of H$_2$O$_2$. Results showed that the por-CeO$_2$ NPs and por-CeO$_2$ NRs had a high affinity for TMB compared with HPR, pure CeO$_2$ NPs, and pure CeO$_2$ NRs, respectively. Simultaneously, por-CeO$_2$ NRs had a high affinity for TMB compared to por-CeO$_2$ NPs. Accordingly, under the identical conditions, por-CeO$_2$ NPs or por-CeO$_2$ NRs had high catalytic activity compared to commercial CeO$_2$ NPs or CeO$_2$ NRs and pure CeO$_2$ NPs or CeO$_2$ NRs, respectively. Based on the peroxidase-like activity of por-CeO$_2$ NPs and por-CeO$_2$ NRs, the authors developed two colorimetric biosensor for the detection of glucose. The linear ranges for glucose were from 4.0×10^{-5} mol L^{-1} to 1.5×10^{-4} mol L^{-1} and 5.0×10^{-5} mol L^{-1} to 1.0×10^{-4} mol L^{-1}, and the LODs were 1.9×10^{-5} mol L^{-1} and 3.3×10^{-5} mol L^{-1}, respectively. Metal doping to improve the peroxidase-like activity of cerium oxide and further enhancement of the sensitivity and detection limit in glucose was also reported by many groups.[88,89] Jampaiah et al.[88] and Song et al.[89] reported the Fe-doped CeO$_2$ NRs (Fe/CeO$_2$ NRs) and the Mo-doped CeO$_2$ NPs (Mo/CeO$_2$ NPs), respectively. The peroxidase-like activity of Fe/CeO$_2$ NRs and Mo/CeO$_2$ NPs were assessed by the catalytic oxidation of substrate TMB in the presence of H$_2$O$_2$. Results showed that those metal-doped cerium oxide had a high catalytic activity compare to pure cerium oxide under the identical conditions. The enhanced peroxidase-like activity of those metal-doped cerium oxide can be attributed to the formation of higher amount of surface defect of Ce^{3+} ions and oxygen vacancies due to the metal doping. Furthermore, as for Fe doping, the presence of Fe^{3+} ions can be also contributed to catalyze H$_2$O$_2$. As for Mo doping, Mo/CeO$_2$ NPs have a small size and a bigger pore radius which show a high catalytic activity. Based on the peroxidase-like activity of Fe/CeO$_2$ NRs and Mo/CeO$_2$ NPs, the authors developed colorimetric biosensor for the detection of glucose. The linear range of Fe/CeO$_2$ NRs and Mo/CeO$_2$ NPs was from 5×10^{-7} to 5×10^{-5} mol L^{-1} and 1×10^{-6} to 1×10^{-4} mol L^{-1}, and the LOD was 3.41×10^{-6} mol L^{-1} and 4×10^{-7} mol L^{-1}, respectively.

Vanadium oxides, mainly including VO$_2$, V$_2$O$_3$, and V$_2$O$_5$, have been extensively studied for their catalysts, electrochemical properties, photocatalysts, surface-enhanced Raman scattering and field emission. The first application of peroxidase-like activity of vanadium oxides (VO$_2$) for colorimetric biosensing of glucose was reported by Wang et al. in 2014.[97] In the work, they investigated VO$_2$ (B) nanobelts that were obtained through a simple one-step hydrothermal route for their intrinsic peroxidase activity to catalyze the oxidation of the typical substrate TMB in the presence of H$_2$O$_2$ to generate a blue color. Results showed that the VO$_2$ (B) nanobelts had a high affinity to H$_2$O$_2$ compared to HPR. Based on the peroxidase-like activity of VO$_2$ (B) nanobelts, the authors developed colorimetric biosensor for the detection of glucose. The linear range for glucose was from 2×10^{-6} to 1.2×10^{-4} mol L^{-1}, and the LOD was as low as 6.5×10^{-7} mol L^{-1}. Owing to the shape, size, and surface chemistry of nanomaterials can dramatically influence their catalytic activities. A comparative study of peroxidase-like activity of VO$_2$ nanomaterials with different morphologies (nanofibers, nanosheets, and nanorods) was reported by Qi et al.[96] The peroxidase-like activity of various VO$_2$ nanomaterials was investigated upon catalysis of H$_2$O$_2$ with peroxidase substrate

TMB. Results showed that the VO$_2$ nanofibers showed a higher affinity for H$_2$O$_2$ than VO$_2$ nanosheets, VO$_2$ nanorods, Fe$_3$O$_4$ MNPs, and HRP. Moreover, the VO$_2$ nanofibers display the highest peroxidase activity compared to VO$_2$ nanosheets and VO$_2$ nanorods. Finally, a comparative colorimetric biosensing of glucose was done on nanofibers, nanosheets, and nanorods. The LOD of the VO$_2$ nanofibers, nanosheets, and nanorods was found to be 9×10^{-6} mol L^{-1}, 3.48×10^{-4} mol L^{-1}, and 4.37×10^{-4} mol L^{-1}, respectively. The VO$_2$ nanofibers, nanosheets, and nanorods showed the linear range from 1.0×10^{-5} to 1.0×10^{-3} mol L^{-1}, 6.25×10^{-4} to 1.5×10^{-2} mol L^{-1}, and 6.25×10^{-4} to 1.0×10^{-2} mol L^{-1}, respectively.

Other metal oxide nanomaterials such as MnO$_2$ nanowires,[94] V$_2$O$_5$ nanowires,[98] NiO NPs and NiC$_{O2}$O$_4$ mesoporous spheres[166] are confirmed to possess intrinsic peroxidase-like activity and used to fabricate colorimetric glucose biosensor as well (see **Table 3**). Those peroxidase-like of metal oxides-based nanomaterials are show a good selectivity and sensitivity for the detection of glucose.

3.4. Metal Nanomaterial-Based Glucose Biosensor

The peroxidase-like activity of the Au NPs and its application for colorimetric determination of glucose was first reported by Li et al. in 2010.[104] In this study, they revealed that the citrate-capped Ag NPs had no catalytic activities, and the peroxidase activity of citrate-capped Au NPs was lower than that of (+) Au NPs. The (+) Au NPs showed a linear range from 1.8×10^{-5} mol L^{-1} to 1.0×10^{-4} mol L^{-1} and with a LOD of 4×10^{-6} mol L^{-1} for the colorimetric biosensing of glucose. More recently, Jiang et al. reported that the peroxidase-like activity of the chitosan-Au NPs and its application for colorimetric glucose biosensor.[111] Results showed that the peroxidase-like activity of chitosan-Au NPs was higher than that of HPR and effective during a broad temperature range between 10–90 °C. The chitosan-Au NPs showed a linear range from 6×10^{-6} mol L^{-1} to 1.40×10^{-4} mol L^{-1} and with a LOD of 3×10^{-6} mol L^{-1} for the colorimetric biosensing of glucose. Au NCs were also applied to the colorimetric biosensing of glucose based on its peroxidase-like activity.[105] Jiang et al. reported that apoferritin-coated Au NCs could efficiently catalyze the substrate TMB by H$_2$O$_2$ to produce a blue color reaction. The kinetic parameters displayed that the apoferritin-coated Au NCs showed higher affinity and catalyst activity for TMB than HPR. Based on the peroxidase-like activity of Au NCs, the Au NCs had a linear range from 2×10^{-3} mol L^{-1} to 1.0×10^{-1} mol L^{-1} for the colorimetric biosensing of glucose. Next, in 2012, Huang et al. found the Ag NPs possess peroxidase-like activity as well and applied to the colorimetric glucose biosensor.[112] The chitosan stabilized Ag NPs (chi-Ag NPs) can efficiently catalyze the substrate OPD and TMB by H$_2$O$_2$ to generate an orange-red and blue color reaction, respectively. Results showed that the chi-Ag NPs exhibited high affinity, pH and thermal durance for TMB compared to HPR. Based on the peroxidase-like activity of chi-Ag NPs, the chi-Ag NPs showed a linear range from 5×10^{-6} mol L^{-1} to 2.0×10^{-4} mol L^{-1} and a LOD of 1.0×10^{-7} mol L^{-1} for the colorimetric biosensing of glucose. More recently, Karim et al.[113] reported a novel nanostructured silver fabric

Table 3. Glucose detection with peroxidase-like of metal oxide nanomaterials.

Metal oxide nanomaterials	Features of catalytic reactions	Comments	Optimum pH	Linear range [μM]	LOD [μM]	Reference
Water-soluble CuO NPs	The catalytic activity of the water-soluble CuO NPs was about 100 times that of the commercial CuO NPs	Substrate: TMB	6.0	100–8000	—	[81]
CuO NPs	CuO NPs break up the O—O bond of H_2O_2 into two •OH	Substrate: terephthalic acid; Glucose in serum samples was tested; Fluorescent detection of glucose	7.0	3–100	1	[82]
Zn-doped CuO NPs	The CuO crystals doped with Zn^{2+} ions generates more •OH in comparison to ZnO or CuO	Substrate: TMB; Glucose in urine samples was tested; Selectivity against sugars: fructose, galactose, and maltose	5.0	25–500	1.5	[83]
CeO_2 NPs	The electron transfers from the CeO_2 NPs to H_2O_2 induce the catalytic oxidation of TMB	Substrate: TMB; Glucose in serum samples was tested; Selectivity against sugars: fructose, mannitol, and maltose	4.0	6.6–130	3	[85]
Porphyrin functionalized CeO_2 NPs	The peroxidase-like activity of the Por-CeO_2 NPs originates from •OH generation; The synergetic effect between porphyrin and CeO_2	Substrate: TMB; Selectivity against sugars: fructose, lactose, mannitol, sucrose, and maltose	3.8	40–150	19	[86]
Mo-doped CeO_2 NPs	The catalytic activity of Mo-doped CeO_2 NPs was much higher than that of pure CeO_2 NPs; Mo doping induce high amount of surface defects causing the more •OH generation	Substrate: TMB; Glucose in serum samples was tested; Selectivity against sugars: fructose, sucrose, and maltose	4.0	0.5–50	0.4	[89]
Fe-doped CeO_2 nanorods	Fe doping induce a high amount of surface defects; Fe^{3+} ions can also contribute toward TMB oxidation	Substrate: TMB; Glucose in serum samples was tested	4.0	1–100	3.41	[88]
Porphyrin functionalized CeO_2 nanorods	The peroxidase-like activity of the Por-CeO_2 originates from •OH generation; The catalytic activity of the Por-CeO_2 nanorods is higher than that of commercial CeO_2 and CeO_2 nanorods	Substrate: TMB; Selectivity against sugars: fructose, lactose, sucrose, and mannitol	3.8	50–100	33	[87]
Co_3O_4 NPs	The peroxidase-like activity of the Co_3O_4 NPs originates from their ability of electron transfer between reducing substrates and H_2O_2, not from •OH generation	Substrate: TMB	5.0	10–1000	5	[93]
Co_3O_4 NPs	The peroxidase-like activity of Co_3O_4 NPs result from the high redox potential of Co^{3+}/Co^{2+}	Substrate: TMB; Selectivity against sugars: fructose, galactose, and maltose		20–200	5	[90]
Porphyrin functionalized Co_3O_4 NPs	The peroxidase-like activity of the Por-Co_3O_4 NPs originates from •OH generation	Substrate: TMB; Selectivity against sugars: fructose, lactose, sucrose, and maltose	3.8	1–10	0.86	[92]
VO_2 (B) nanobelts	—	Substrate: TMB	5.0	2–120	0.65	[97]
V_2O_5 nanowires	—	Substrate: TMB	4.0	1–500	1	[98]
VO_2 nanofibers	VO_2 nanofibers exhibited the best peroxidase-like activity	Substrate: TMB	4.0	10–10 000	9	[96]
VO_2 nanosheets		Substrate: TMB	4.0	625–15 000	348	[96]
VO_2 nanorods		Substrate: TMB	4.0	625–10 000	437	[96]
VO_3-ordered mesoporous carbon	—	Substrate: ABTS; Glucose in serum samples was tested	4.0	10–4000	3.3	[100]

ADVANCED
SCIENCE NEWS
www.advancedsciencenews.com

NANO · MICRO
small
www.small-journal.com

Table 3. Continued.

Metal oxide nanomaterials	Features of catalytic reactions	Comments	Optimum pH	Linear range [μM]	LOD [μM]	Reference
MnO_2 nanowires	The peroxidase-like activity of the MnO_2 nanowires originates from their ability of electron transfer between reducing substrates and H_2O_2, not from •OH generation	Substrate: ABTS	3.5	10–2000	2	[94]
MnO_2 nanosheets	Mn^{2+} play an important role in catalytic reactions	No need of substrate; Glucose in serum samples was tested	8.4–10.4	0.5–50	0.17	[95]
$NiCo_2O_4$ mesoporous spheres	The peroxidase-like activity of $NiCo_2O_4$ MS originated from not only •OH but also $^1O_2$ for the oxidation of TMB	Substrate: TMB; Glucose in serum samples was tested	4.0	2–100	1.62	[166]
Porphyrin modified NiO NPs	The peroxidase-like activity of Por–NiO NPs originated from the generation of •OH	Substrate: TMB; Glucose in serum samples was tested; Selectivity against sugars: fructose, lactose, sucrose, and maltose	3.8	50–500	20	[101]

(nano-Ag@fabric) for the colorimetric biosensing of glucose based on its peroxidase-like activity. The nano-Ag@fabric can efficiently catalyze the substrate ABTS, OPD, and TMB by H_2O_2 to generate green, orange-red, and blue color reactions, respectively. Based on the peroxidase-like activity of nano-Ag@fabric, the nano-Ag@fabric showed a linear range from 1.0×10^{-4} mol L^{-1} to 2×10^{-3} mol L^{-1} and a LOD of 8.0×10^{-5} mol L^{-1} for the colorimetric biosensing of glucose.

The application of copper nanomaterials (Cu NCs) for colorimetric biosensing of glucose was reported by Xu and his groups in 2013 by using the peroxidase-like activity.[120] The bovine serum albumin (BSA) is as a reducer and stabilizer to synthesize water-soluble Cu NCs. As described in Section 2.4, the Cu NCs possessed a peroxidase-like activity. Based on the peroxidase-like activity of Cu NCs, the Cu NCs showed a linear range from 1.0×10^{-4} mol L^{-1} to 2×10^{-3} mol L^{-1} and a LOD of 1.0×10^{-4} mol L^{-1} for the colorimetric biosensing of glucose. The peroxidase-like activity of the Cu NPs and its application for colorimetric biosensing of glucose was reported Ai et al.[119] In this report, the authors prepared the stable Cu NPs through a facile annealing process using humic acid as the reductant and stabilizer. The as-prepared Cu NPs indicate excellent stability which can use to oxidize even after 6 months. More importantly, the result displayed that the Cu NPs had significantly higher affinity and catalyst activity for TMB than HPR. Based on the peroxidase-like activity of Cu NPs, the Cu NPs showed a linear range from 1.0×10^{-6} mol L^{-1} to 1.0×10^{-4} mol L^{-1} and a LOD was as low as 6.86×10^{-7} mol L^{-1} for the colorimetric biosensing of glucose. Platinum nanomaterials mimic peroxidase was first reported in 2011.[115] But its application for colorimetric detection of glucose was first reported by Jin et al. in 2017.[114] In the works, the Pt NCs showed excellent water solubility which was prepared by using yeast extract as stabilizing and reducing agents. The Pt NCs can efficiently catalyze the substrate TMB by H_2O_2. Based on the peroxidase-like activity of Pt NCs, the Pt NCs displayed a linear range from 0 to 2.0×10^{-4} mol L^{-1} μM and a LOD was as low as 2.8×10^{-7} mol L^{-1} for the colorimetric biosensing of glucose. Rh NPs were also reported to possess peroxidase-like activity and applied to the colorimetric biosensing of glucose.[118]

The application of bimetallic nanomaterials for fabricate colormetric glucose biosensor based on the peroxidase-like activity were reported by many groups as well.[121,123,127–129] For examples, Huang et al.[123] reported that Fe–Co bimetallic alloy nanoparticles (Fe–Co NPs) possessed highly peroxidase-like activity and its application for glucose biosensor. Compared with noble-based bimetallic NPs, this Fe–Co NPs show low-cost. The Fe–Co NPs can efficiently catalyze the substrate TMB in the presence of H_2O_2. Results revealed that the Fe–Co NPs had high affinity to H_2O_2 compared to Fe NPs and Co NPs therefore the activity of the Fe–Co NPs was remarkably enhanced. Based on the peroxidase-like activity of Fe–Co NPs, the authors developed a colorimetric biosensor for the biosensing of glucose. The linear range for glucose was from 5.0×10^{-7} mol L^{-1} to 1.0×10^{-5} mol L^{-1} and the LOD was as low as 1.0×10^{-8} mol L^{-1}. The peroxidase-like activity of Au@Ag heterogeneous nanorods (Au@Ag NRs) and its application for glucose biosensor was reported by Han and co-workers.[127] The peroxidase mimetics of Au@Ag NRs is based on catalyze the substrate ABTS in the presence of H_2O_2. Results exhibited that the Au@Ag NRs displayed long-term storage stability and excellent temperature stability. Based on the peroxidase-like activity of Au@Ag NRs, the authors developed a colorimetric biosensor for the detection of glucose. The developed colorimetric glucose biosensor had a linear range from 5.0×10^{-5} mol L^{-1} to 2.0×10^{-2} mol L^{-1} and a LOD of 2.5×10^{-5} mol L^{-1}.

Other bimetallic nanomaterials such as Au@Ag core–shell NPs and Au@Pt NRs are confirmed to possess intrinsic peroxidase-like activity and used to fabricate colorimetric glucose biosensor as well (see **Table 4**).

3.5. Metal Sulfide Nanomaterials-Based Glucose Biosensor

The peroxidase-like activity of the MoS_2 NSs and its application for colorimetric biosensing of glucose was reported by Guo et al. in 2014 for the first time.[134] The peroxidase-like activity of the MoS_2 NSs had been described in Section 2.5. Based on the peroxidase-like activity of the MoS_2 NSs, the authors developed a colorimetric biosensor for the detection of glucose. The

Table 4. Glucose detection with peroxidase-like of metal nanomaterials.

Metal nanomaterials	Features of catalytic reactions	Comments	Optimum pH	Linear range [μM]	LOD [μM]	Reference
Positively charged Au NPs	(+)Au NPs break up the O—O bond of H_2O_2 into two •OH	Substrate: TMB; Selectivity against sugars: maltose, lactose, and fructose	4.0	18–1100	4	[104]
Chitosan-Au NPs	—	Substrate: TMB; Glucose in serum samples was tested	4.2	6–140	3	[111]
Rhodium nanoparticles	Rh NPs facilitate the electron transfer between TMB and H_2O_2 and catalyze the decomposition of H_2O_2 into •OH	Substrate: TMB; Glucose in serum samples was tested	4.0	5–125	0.75	[118]
Apoferritin paired gold clusters	The peroxidase-like activity of the Au–Ft originates from •OH generation; The catalytic activity decreases upon disassembly of apoferritin nanostructures	Substrate: TMB; Glucose in serum samples was tested; Selectivity against sugars: maltose, lactose, and fructose	4.0	2000–10 000	-	[105]
Chitosan-Ag NPs	The peroxidase-like activity of the chitosan–AgNPs originates from •OH generation	Substrate: TMB; Glucose in serum samples was tested	3.0	5–200	0.1	[112]
Cu NPs	—	Substrate: TMB; Glucose in serum samples was tested; Selectivity against sugars: maltose, lactose, and fructose	3.0	1–100	0.686	[119]
Pt nanoclusters	The peroxidase-like activity of the Pt NCs originates from their ability of electron transfer between reducing substrates and H_2O_2, not from •OH generation	Substrate: TMB; Glucose in serum samples was tested; Selectivity against sugars: maltose, sucrose, lactose, and fructose	5.0	0–200	0.28	[114]
Cu nanoclusters	Cu NCs break up the O—O bond of H_2O_2 into two •OH; Cu^{2+} contribute to the catalytic reaction	Substrate: TMB; Selectivity against sugars: maltose, lactose, and fructose	4.0	100–2000	100	[120]
Au/Ag nanobelts	The peroxidase-like activity of Au/Ag nanobelts could be tuned by AuNP/Ag ratio	Substrate: TMB	7.0	100–7400	85	[129]
Au@Ag core–shell NPs	—	Substrate: TMB; Selectivity against sugars: maltose, lactose, and fructose	4.5	0–0.2 1–100	0.01	[128]
Au@Ag nanorods	The catalytic activity of Au@Ag NRs at pH 6.5	Substrate: ABTS; Glucose in serum samples was tested	6.5	50–2000	25	[127]
Au@Pt core/shell nanorods	Au@Pt core/shell nanorod exhibited dual functional enzyme-like (peroxidase and oxidase-like) activities	Substrate: TMB; Selectivity against sugars: maltose, lactose, and fructose	4.5	45–400	45	[121]
Nanostructured silver fabric	The peroxidase-like activity of the nanostructured silver fabric originates from •OH generation	Substrate: TMB; Glucose in urine samples was tested; Selectivity against sugars: maltose, sucrose, lactose, and fructose	5.0	100–2000	80	[113]
Fe–Co bimetallic NPs	The peroxidase-like activity of the Fe–Co bimetallic NPs originates from •OH generation	Substrate: TMB; Glucose in serum samples was tested; Selectivity against sugars: maltose, lactose, and fructose	4.0	0.5–10	0.01	[123]

developed colorimetric glucose biosensor had a linear range from 5.0×10^{-6} mol L^{-1} to 1.5×10^{-4} mol L^{-1} and a LOD of 1.2×10^{-6} mol L^{-1}. The peroxidase-like activity of the MoS_2 NPs and its application for colorimetric detection of glucose was reported by many groups.[133,136,138] Bare MoS_2 NPs are difficult to dissolve in water, a suitable surface modification can provide good dispersion and stability of MoS_2 NPs. Based on this discovery, Xian et al. prepared surfactant modified MoS_2 NPs and investigated the peroxidase-like activity of the different types of MoS_2 NPs.[138] They found that the sodium dodecyl sulfate (SDS) modified MoS_2 NPs (SDS-MoS_2 NPs) possessed high peroxidase-like activity toward TMB compared to cation surfactant,

cetyltrimethyl ammonium bromide (CTAB) modified MoS_2 NPs (CTAB-MoS_2 NPs). This can be attributed to the negatively charged SDS–MoS_2 NPs have high affinity toward the positivity charged TMB. Based on the peroxidase-like activity of the SDS-MoS_2 NPs, the authors developed a colorimetric biosensor for the determination of glucose. The developed colorimetric glucose biosensor had a linear range from 5×10^{-6} mol L^{-1} to 5.0×10^{-4} mol L^{-1} and a LOD of 5.7×10^{-7} mol L^{-1}. Polyvinylpyrrolidone (PVP) modified MoS_2 NPs (PVP-MoS_2 NPs) was also reported possessed enhanced peroxidase-like activity and used to colorimetric biosensing of glucose.[133] The PVP surfactant can induce the generation of small size of MoS_2 NPs ($\approx$5 nm).

**ADVANCED
SCIENCE NEWS**
www.advancedsciencenews.com

NANO · MICRO
small
www.small-journal.com

The peroxidase-like activity of the PVP-MoS$_2$ NPs was examined by the catalytic oxidation of the peroxidase substrate TMB in the presence of H$_2$O$_2$. Based on the peroxidase-like activity of the PVP–MoS$_2$ NPs, the authors fabricated a colorimetric biosensor for the determination of glucose. The developed colorimetric glucose biosensor had a linear range from 1.0×10^{-3} mol L^{-1} to 1.0×10^{-2} mol L^{-1} and a LOD of 3.2×10^{-4} mol L^{-1}.

More recently, Zhao et al. reported a mixed-solvent (ethanol/water) liquid exfoliated MoS$_2$ NPs as peroxidase-like for colorimetric biosensing of glucose.[136] Compared with hydrothermal method, which requires high pressure and temperature, this liquid exfoliation method is simple and can produce high purity of MoS$_2$ NPs. Results indicated that the MoS$_2$ NPs had high affinity to H$_2$O$_2$ compared to HPR. Based on the peroxidase-like activity of the MoS$_2$ NPs, a colorimetric biosensor was developed for the biosensing of glucose. The developed colorimetric glucose biosensor had a linear range from 1.5×10^{-5} mol L^{-1} to 1.35×10^{-4} mol L^{-1} and a LOD of 7×10^{-6} mol L^{-1}. The peroxidase-like of MoS$_2$ NFs and its application for colorimetric determination of glucose was reported by Gu et al.[135] This work further demonstrated that the surface modification and electrostatic affinity between nanomaterials and substrate played a key role in catalytic reaction. They found that the positively/negatively charged cysteine (Cys) modified MoS$_2$ NFs (Cys-MoS$_2$ NFs) possessed the highest peroxidase activity compared with positively charged polyethyleneimine (PEI), neutrally charged polyvinylpyrrolidone (PVP), and negatively charged polyacrylic acid (PAA) modified MoS$_2$ NFs either for catalyze TMB or ABTS. Moreover, the peroxidase activity of Cys-MoS$_2$ NFs/ABTS system was higher than that of the Cys-MoS$_2$ NFs/TMB system. Based on high peroxidase-like activity of the Cys-MoS$_2$ NFs, a colorimetric biosensor was developed for the detection of glucose. The developed colorimetric glucose biosensor had a linear range from 5.0×10^{-5} mol L^{-1} to 1.0×10^{-3} mol L^{-1} and a LOD of 3.35×10^{-5} mol L^{-1}.

Other metal sulfide nanomaterials including WS$_2$ NSs and ZnS NPs were reported for colorimetric biosensing of glucose based on its peroxidase-like activity as well. Guo et al. first reported that WS$_2$ NSs possessed intrinsic peroxidase-like activity and applied to colorimetric biosensing of glucose in 2014.[142] The WS$_2$ NSs can catalyze the oxidation of substrate TMB, ABTS and OPD to generate color reaction in the presence of H$_2$O$_2$. Results showed that the WS$_2$ NSs had high catalytic activity to H$_2$O$_2$ compared with HPR. On the basis of high peroxidase-like activity of the WS$_2$ NSs, a colorimetric biosensor was developed for the biosensing of glucose. The developed colorimetric glucose biosensor had a linear range from 5.0×10^{-6} mol L^{-1} to 3.0×10^{-4} mol L^{-1} and a LOD was as low as 2.9×10^{-6} mol L^{-1}. Recently, Liu et al. reported that ZnS NPs possessed intrinsic peroxidase-like activity and applied to colorimetric detect glucose for the first time.[140] Based on previous works, the ZnS NPs was modified with porphyrins (por-ZnS NPs) to enhance the catalytic activity of ZnS NPs. In the presence of H$_2$O$_2$, the peroxidase-like activity of the ZnS NPs was evaluated by catalytic oxidation of the substrate TMB. Results indicated that the por-ZnS NPs had a higher affinity for TMB than pure ZnS NPs and HPR. Based on the peroxidase-like activity of the por-ZnS NPs, a colorimetric biosensor was developed for the detection of glucose. The developed colorimetric

glucose biosensor had a linear range from 5.0×10^{-5} mol L^{-1} to 5.0×10^{-4} mol L^{-1} and a LOD was as low as 3.6×10^{-5} mol L^{-1}. The colorimetric glucose biosensor based on peroxidase-like of metal sulfide nanomaterials are summarized in **Table 5**.

3.6. Nanocomposites-Based Glucose Biosensor

Chen et al.[146] reported that the GO–Fe$_3$O$_4$ MNPs nanocomposites possessed peroxidase-like activity and applied to colorimetric detect glucose. The as-prepared GO–Fe$_3$O$_4$ MNPs nanocomposites retain the magnetic properties of Fe$_3$O$_4$ MNPs. The GO–Fe$_3$O$_4$ MNPs nanocomposites can catalyze the oxidation of substrate TMB to generate color reaction in the presence of H$_2$O$_2$. Results revealed that the nanocomposites showed high catalytic activity to H$_2$O$_2$ compared to pure Fe$_3$O$_4$ MNPs. Based on the peroxidase-like activity of the GO–Fe$_3$O$_4$ MNPs nanocomposites, a colorimetric biosensor was developed for the biosensing of glucose. The developed colorimetric glucose biosensor had a linear range from 2×10^{-6} mol L^{-1} to 2.0×10^{-4} mol L^{-1} and a LOD was as low as 7.4×10^{-7} mol L^{-1}. Fe$_3$O$_4$@C nanocomposites with enhanced peroxidase-like activity for colorimetric biosensing of glucose was reported by Tan and co-workers.[145] This developed colorimetric biosensor had a linear range from 6×10^{-6} mol L^{-1} to 1.0×10^{-4} mol L^{-1} and a LOD was as low as 2×10^{-6} mol L^{-1}. Other MNPs-based nanocomposites with enhanced peroxidase-like activity to fabricate colorimetric glucose biosensors are summarized in **Table 6**.

Pt–Ag/MoS$_2$ nanocomposites[151] with enhanced peroxidase-like activity for colorimetric biosensing of glucose was reported by Yang et al. The peroxidase-like activity of Pt–Ag/MoS$_2$ nanocomposites was investigated by catalytic oxidation substrate TMB, ABTS, and OPD in the presence of H$_2$O$_2$. Compared with Pt–Ag NPs and MoS$_2$ sheets, Pt–Ag/MoS$_2$ nanocomposites exhibited enhanced peroxidase-like activity. This can be attributed to Pt–Ag/MoS$_2$ nanocomposites not only provide abundant active sites for the adsorption of TMB, but equip with large surface area. Based on the peroxidase-like activity of the Pt–Ag/MoS$_2$ nanocomposites, a colorimetric biosensor was developed for the detection of glucose. The developed colorimetric glucose biosensor had a linear range from 1.0×10^{-6} mol L^{-1} to 1.0×10^{-5} mol L^{-1} and a LOD was as low as 8.0×10^{-7} mol L^{-1}. More recently, Weng et al.[152] reported that the GO/MoS$_2$ hybrid possessed enhanced peroxidase-like activity and applied to colorimetric biosensing of glucose. Enzyme kinetics experiments revealed that the apparent K_m value of GO/MoS$_2$ hybrid with H$_2$O$_2$ as the substrate was 770 times lower than that of Fe$_3$O$_4$ MNPs and 18.5 times lower than that of HRP. In this work, the authors further demonstrated that visible and infrared lights could promoted the synergistic effect of two components in GO/MoS$_2$ nanocomposites to improve its peroxidase-like activity. Based on the peroxidase-like activity of the GO/MoS$_2$ nanocomposites, a colorimetric biosensor was developed for the detection of glucose. The developed colorimetric glucose biosensor had a linear range from 1.0×10^{-6} mol L^{-1} to 5.0×10^{-5} mol L^{-1} and a LOD of 8.3×10^{-7} mol L^{-1} without light and 8.6×10^{-8} mol L^{-1} under visible light. The 8.6×10^{-8} mol L^{-1} was the lowest LOD based on the peroxidase-like activity of nanomaterials for colorimetric glucose biosensors.

ADVANCED
SCIENCE NEWS
www.advancedsciencenews.com

NANO · MICRO
small
www.small-journal.com

Table 5. Glucose detection with peroxidase-like of metal sulfide nanomaterials.

Metal sulfide nanomaterials	Features of catalytic reactions	Comments	Optimum pH	Linear range [μM]	LOD [μM]	Reference
MoS_2 nanosheets	MoS_2 nanosheets facilitate the electron transfer between TMB and H_2O_2, and catalyze the decomposition of H_2O_2 into •OH	Substrate: TMB; Glucose in serum samples was tested	6.9	5–150	1.2	[134]
Sodium dodecyl sulfate modified MoS_2 NPs	The electron transfer from the MoS_2 NPs to H_2O_2, thus increasing the reaction rate of TMB oxidation by H_2O_2	Substrate: TMB; Glucose in serum samples was tested; Selectivity against sugars: fructose, sucrose, and galactose	6.78	5–500	0.57	[138]
Polyvinylpyrrolidone modified MoS_2 NPs	The peroxidase-like activity of the PVP-MoS_2 NPs originates from •OH generation	Substrate: TMB; Selectivity against sugars: fructose, lactose, and maltose Cytotoxicity of PVP-MoS_2 NPs was evaluated	4.0–5.0	1000–10 000	320	[133]
MoS_2 NPs	MoS_2 NPs absorb TMB facilitate the electron transfer to H_2O_2 and promote catalyze the decomposition of H_2O_2 into •OH	Substrate: TMB; Selectivity against sugars: fructose, lactose, and sucrose	3.5	15–135	7	[136]
MoS_2 nanoflakes	Cysteine modified MoS_2 NFs showed the highest catalytic activity; The peroxidase-like activity of the MoS_2 NFs originates from •OH generation	Substrate: ABTS	4.0	50–1000	33.51	[135]
Porphyrin modified ZnS NPs	The peroxidase-like activity of the Por-ZnS NPs originates from •OH generation	Substrate: TMB; Selectivity against sugars: maltose, lactose, and sucrose	3.8	50–500	36	[140]
WS_2 nanosheets	—	Substrate: TMB; Glucose in serum samples was tested	6.9	5–300	2.9	[142]
VS_2 nanosheets	The peroxidase-like activity of the VS_2 nanosheets originates from •OH generation	Substrate: TMB; Glucose in food samples was tested; Selectivity against sugars: fructose, maltose, lactose, and sucrose	4.0	5–250	1.54	[141]
CuS NPs	Cu^{2+} ion acts as Fenton-like reagent and interact with the substrate by catalyzing the decomposition of H_2O_2 into •OH	Substrate: TMB; Glucose in serum samples was tested	4.0	2–1800	0.12	[180]

Other nanocomposites with enhanced peroxidase-like activity for colorimetric biosensing of glucose were reported by many groups as well. Such as, $TiO_2@CeO_x$ core–shell nanoparticles,[153] MnSe loaded g-C_3N_4 nanocomposite,[154] Au@Ag–hemin decorated reduced graphene oxide sheets,[155] Cu–Ag bimetallic nanoparticles decorated reduced graphene oxide sheets,[156] graphene quantum dots–copper oxide nanocomposites (GQDs/CuO),[158] TiO_2-encapsulated Au (Au@TiO_2) yolk–shell nanostructure,[159] and $CoSe_2$/reduced graphene oxide ($CoSe_2$/rGO) hybrid[160] (see Table 6). Those enhanced peroxidase-like activity of nanocomposites fabricated colorimetric glucose biosensors usually exhibits low detection limit.

3.7. Nonenzymatic Colorimetric Glucose Biosensor

Recently, gold nanoparticles (Au NPs) also have been found to possess glucose oxidase-like activity.[167–170] The authors discovered that the "naked" Au NPs can be capable of catalytically

oxidizing glucose to produce gluconic acid and hydrogen peroxide.[167] Thus, some research groups have been designed dual enzyme-like activities nanomaterials by combing the glucose oxidase-like activity of AuNPs and peroxidase-like activity of nanomaterials.[171–174] Those dual enzyme-like activities nanomaterials is described as "tandem nanozyme." By combing the GOx-like activity of AuNPs and peroxidase-like activity of nanomaterials, some nonenzymatic glucose colorimetric detection systems have been successfully developed (see **Table 7**).[171,172,174] He et al. reported a novel enzymatic cascade system based on Fe_3O_4–Au@mesoporous SiO_2 microspheres with both high GOx and peroxidase-mimic activities in 2013.[174] In this "tandem nanozyme," the high peroxidase-mimic activity is provided by magnetic Fe_3O_4 cores and make the tandem nanozyme system easily recyclable. Ultrafine Au NPs are dispersed on the surface of Fe_3O_4 cores with high GOx-mimic activity. Moreover, Fe_3O_4–Au particles are embedded in mesoporous SiO_2 shells to prevent the aggregation and maintain the stability of "tandem nanozyme" even under harsh conditions. Meanwhile,

Table 6. Glucose detection with peroxidase-like of nanocomposites.

Nanocomposites	Features of catalytic reactions	Comments	Optimum pH	Linear range [µM]	LOD [µM]	Reference.
Graphene oxide–Fe_3O_4 magnetic nanocomposites	The nanocomposites exhibited much higher activity than GO alone or Fe_3O_4 alone	Substrate: TMB; Glucose in urine samples was tested; Selectivity against sugars: maltose, lactose, and fructose	4.0	2–200	0.74	[146]
g-C_3N_4–Fe_3O_4 magnetic nanocomposites	The nanocomposites exhibited much higher activity than g-C_3N_4 alone or Fe_3O_4 alone	Substrate: TMB; Glucose in serum samples was tested; Selectivity against sugars: maltose, lactose, and fructose	4.0	1–140	0.25	[149]
PtAg NPs decorated MoS_2 nanosheets	The peroxidase-like activity of the nanocomposites originates from •OH generation; The nanocomposites not only has larger surface area, but also provides abundant active sites for the adsorption of TMB molecules	Substrate: TMB Selectivity against sugars: mannitol, lactose, and fructose	4.0	1–10	0.8	[151]
MnSe-loaded g-C_3N_4 nanocomposite	The synergetic effects of high conductivity and electron-transfer capability for g-C_3N_4 supports, and intrinsic catalysis activity for MnSe nanocatalysts, facilitated peroxidase-like catalysis	Substrate: TMB; Glucose in serum and food samples was tested; Selectivity against sugars: maltose, lactose, and fructose	4.5	160–1600	8	[154]
Au@Ag–hemin decorated reduced graphene oxide sheets	The peroxidase-like activity of the nanocomposites originates from their ability of electron transfer between reducing substrates and H_2O_2	Substrate: TMB; glucose in serum samples was tested	4.1	2–5	0.425	[155]
Cu–Ag bimetallic NPs decorated reduced graphene oxide nanosheets	The nanocomposites showed high electron transfer, provided larger sites for TMB adsorption	Substrate: TMB; Selectivity against sugars: maltose, lactose and fructose	4.0	1–30	3.82	[156]
Fe_3O_4@SiO_2@Au MNPs	The nanocomposites exhibited much higher activity than free Fe_3O_4 MNPs and BSA-Au NCs	Substrate: TMB; Glucose in serum and food samples was tested; Selectivity against sugars: maltose, lactose, and fructose	3.0	5–350	3.5	[148]
MoS_2/graphene oxide hybrid	The visible and infrared lights could promote the synergistic effect of two components in MoS_2/GO to improve its photocatalytic activity	Substrate: TMB; Glucose in serum samples was tested Selectivity against sugars: maltose, lactose, and fructose	4.0	1–50	0.83 (no light) 0.086 (light)	[152]
Graphene quantum dots–copper oxide nanocomposites	The peroxidase-like activity of the nanocomposites originates from •OH generation	Substrate: TMB; Glucose in serum samples was tested; Selectivity against sugars: mannose, lactose, fructose, and maltose	3.5	2–100	0.59	[158]
Au@TiO_2 yolk–shell nanostructure	The peroxidase-like activity of the nanocomposites originates from •OH generation	Substrate: TMB; Selectivity against sugars: maltose, lactose, and fructose	3.5	0–10	3.5	[159]
$CoSe_2$/reduced graphene oxide nanohybrids	The peroxidase-like activity of the nanocomposites originates from •OH generation	Substrate: TMB; Glucose in serum samples was tested; Selectivity against sugars: sucrose, lactose, fructose, and galactose	4.5	1–1000	0.553	[160]
Magnetic mesoporous silica nanoparticle (Fe_3O_4@MSN)	—	Substrate: TMB; Selectivity against sugars: maltose, lactose, and fructose	5.5	10–500	4	[147]
Copper-incorporated SBA-15	The peroxidase-like activity of the nanocomposites is derived from the Cu incorporation	Substrate: TMB; Glucose in serum samples was tested; Selectivity against sugars: maltose, lactose, and fructose	3.0	2000–80 000	5.4	[181]
Prussian Blue-modified iron oxide nanoparticles	Using the 3,5-di-tert butylcatechol (3,5-DTBC) as new substrate	Substrate: 3,5-di-tert-butylcatechol (3,5-DTBC); Glucose in serum samples was tested	7.0	1–80	0.16	[182]

ADVANCED
SCIENCE NEWS
www.advancedsciencenews.com

NANO · MICRO
small
www.small-journal.com

Table 6. Continued.

Nanocomposites	Features of catalytic reactions	Comments	Optimum pH	Linear range [μM]	LOD [μM]	Reference.
$Cu_2(OH)_3Cl$-CeO_2 nanocomposite	—	Substrate: TMB; Glucose in serum samples was tested	3.0	100–2000	50	[183]
FeOOH and N-doped carbon nanosheets	—	Substrate: TMB; Glucose in urine samples was tested; Selectivity against sugars: sucrose, galactose, and fructose	4.0	8–800	0.2	[184]
Carbon-coated magnetite nanoparticle ($Fe_3O_4@C$)	The peroxidase-like activity of the nanocomposites originates from •OH generation	Substrate: TMB; Glucose in urine, serum samples was tested; Selectivity against sugars: sucrose, mannose, galactose, and fructose	4.5	6–100	2	[145]
MoS_2-decorated $MgFe_2O_4$ nanocomposite	—	Substrate: TMB; Glucose in serum samples was tested; Selectivity against sugars: sucrose, galactose, and fructose	4.0	5–200	2	[185]
$Co_3O_4@CeO_2$ hybrid flower-like microspheres	The oxygen vacancies and the facilitated electron transfer enhanced the catalytic activity	Substrate: TMB; Selectivity against sugars: maltose, lactose, and fructose	4.0	1–75	1.9	[186]
Fe–porphyrin-based covalent organic framework	The peroxidase-like activity of the nanocomposites originates from •OH generation	Substrate: TMB; Selectivity against sugars: maltose, lactose, and sucrose	5.0	5–350	1	[187]

mesoporous SiO_2 shells permit small active molecules to spread in and out of its mesoporous. The Fe_3O_4–Au@ mesoporous SiO_2 microspheres as robust nanoreactors can catalyze a spontaneous tandem reaction, which includes oxidation of glucose to generate H_2O_2 and gluconic acid in the presence of oxygen, and then oxidation of TMB by catalyzing the generated H_2O_2 to cause a color change. At the optimal pH value of 4.0, the tandem nanozyme was used to detect glucose. **Figure 5** shows the dual enzyme-like activities of mesoporous silica-encapsulated gold nanoparticles (EMSN-Au NPs) for colorimetric biosensing glucose. The developed colorimetric glucose biosensor had a linear range from 1.0×10^{-5} mol L^{-1} to 1.3×10^{-4} mol L^{-1} and a LOD of 5×10^{-7} mol L^{-1}.

Another tandem nanozyme was reported by Qu et al. in 2014.[172] In this work, the authors constructed a tandem nanozyme by incorporating Au NPs and V_2O_5 nanowires through a facile chemical method. In this tandem nanozyme system, Au NPs provide high GOx-mimic catalytic activity and V_2O_5 nanowires with high peroxidase-mimic activity. Results showed that V_2O_5 nanowires exhibited peroxidase-like activity toward ABTS at pH 4.0, but Au NPs showed their strongest intrinsic GOx-like activity at pH 7.0. The mimicking

dual enzyme cascade reaction of V_2O_5–Au NP nanozyme is performed as follows: a) V_2O_5–Au NP was incubated with glucose and ABTS in pH 7.0. In this process, the Au NPs mimicked GOx in catalyzing the oxidation of glucose to gluconic acid. At the same time, the substrate oxygen was converted into H_2O_2; b) the mixture was then adjusted to pH 4.0, thus V_2O_5 nanowires catalyzed H_2O_2, mimicking peroxidase in the presence of ABTS as peroxidase substrate at pH 4.0 and generating a green color. Based on this principle, authors designed a colorimetric method for the detection of glucose using V_2O_5–Au NP for the enzyme-mimicking cascade reaction. The developed colorimetric glucose biosensor had a linear range from 0 to 1.0×10^{-5} mol L^{-1} and a LOD of 5×10^{-7} mol L^{-1}.

More recently, Zhang et al. reported the bovine serum albumin stabilized Au NPs (Au@BSA NPs) as the "tandem nanozyme" in 2018.[171] GOx simulation experiment showed that Au@BSA NPs can oxidation of glucose to produce gluconic acid and H_2O_2 by oxygen. Meanwhile, peroxidase simulation experiment showed that Au@BSA NPs can oxidation of TMB by catalyzing H_2O_2 to produce a color change. Taken together, these results indicated that Au@BSA NPs simultaneously exhibit GOx-like activity and peroxidase-like activity.

Table 7. Nonenzymatic colorimetric glucose biosensor.

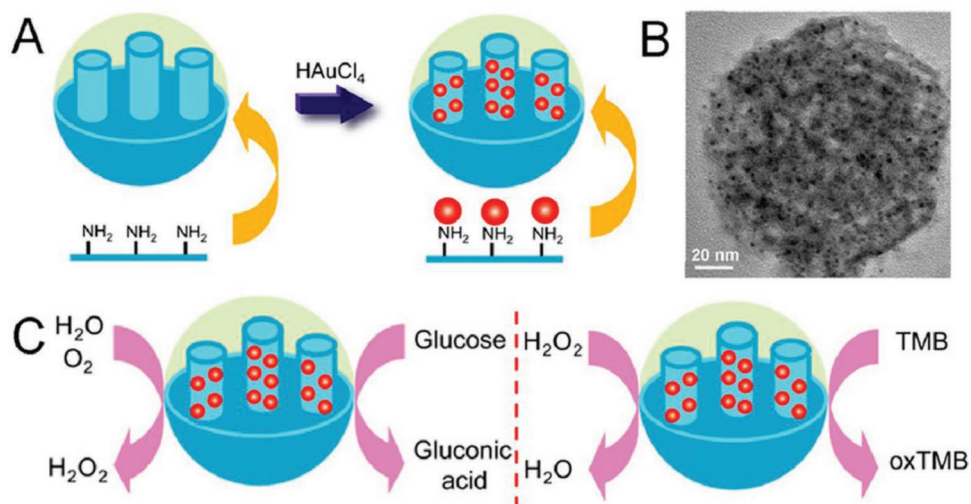| Nanomaterials	Comments	Optimum pH	Linear range [μM]	LOD [μM]	Reference
Fe_3O_4–Au@mesoporous SiO_2 microspheres	Substrate: TMB Do not need GOx	4.0	10–130	0.5	[174]
V_2O_5–Au NP nanocomposites	Substrate: ABTS Do not need GOx	GOx-like activity at pH 7.0 peroxidase-like activity at pH 4.0	0–10	0.5	[172]
Au@BSA NPs–GO nanocomposites	Substrate: TMB Do not need GOx	4.0	1–300	0.6	[171]

Figure 5. A) Schematic illustration for the synthesis of EMSN-Au NPs. B) TEM image of EMSN-Au NPs. C) Schematic illustration for dual enzyme-like activities of EMSN-Au NPs for colorimetric biosensing glucose. Reproduced with permission.[173] Copyright 2014, American Chemical Society.

Interestingly, Au@BSA NPs can simultaneously possess GOx-like activity and peroxidase-like activity at the same pH. Moreover, when Au@BSA NPs modified with GO, the dual enzyme activities of Au@BSA NPs is still not change. According to the GOx-like activity and peroxidase-like activity of Au@BSA NPs–GO, the authors designed a colorimetric method for the detection of glucose. The developed colorimetric glucose biosensor had a linear range from 1.0×10^{-6} to 3.0×10^{-4} mol L^{-1} and a LOD of 6×10^{-7} mol L^{-1}.

4. Tunable Peroxidase-Like Activity of Nanomaterials

Like the HPR, the nanomaterials' peroxidase-like activity can be adjusted and influenced by many factors as well. In this part, several important factors are reviewed and summarized.

4.1. Size

Size-dependence is a key factor which related to many properties of nanomaterials. Unsurprisingly, the peroxidase-like activity of nanomaterials can be possibly tuned by changing their sizes, which has been revealed in many researches.[32,169,175–177] Small nanoparticles usually show high activity compared to the large ones in most cases, likely because of its high surface to volume ratio. For instance, Peng and co-workers demonstrated the size-dependent peroxidase-like catalytic activity of Fe_3O_4 MNPs (**Figure 6**a).[175] By comparing Fe_3O_4 MNPs with different diameters, they revealed that the Fe_3O_4 MNPs' activity decreased with the raising of nanoparticle size.

4.2. Morphology and Shape

The morphology and shape of nanomaterials also hold an important position in tuning their peroxidase-like catalytic activity. In Qi's report,[96] they synthesized vanadium dioxide nanomaterials with different morphologies (nanofibers, nanosheets, and nanorods) and compared their peroxidase-like activities. Simultaneously, a comparative quantitative detections of glucose was done on nanofibers, nanosheets, and nanorods. Under the optimal reaction conditions, the LOD of the VO_2 nanofibers, nanosheets, and nanorods for glucose were found to be 9×10^{-6}, 3.48×10^{-4}, and 4.37×10^{-4} mol L^{-1}, respectively. A further study for a detailed understanding of the shape and morphology effects of Fe_3O_4 MNPs on their peroxidase-like activities was carried by Liu and co-workers (Figure 6b).[178] Compared with octahedrons and triangular plates, the spheres showed the highest catalytic activity, their higher specific surface area was responsible for this difference. For the octahedrons and the triangular plates, which showed similar surface area and size, their surface atom arrangements were responsible for the difference in activity. Compared to the octahedrons, with (111) planes, the higher catalytic activities of the triangular plates were due to the more active (220) planes.

4.3. Surface Modification and Coating

The surface modification and coating of nanomaterials provide them not only changed surface properties for further bioconjugation but also enhanced dispersibility and stability. Thus, coating and modification have been used to further tune the nanomaterials' activities. A number of methods can be attributed to tune the activity, such as the packing density and size of the coating groups and the thickness of the modifying layer. Generally, the surface modification and coating shields the surface of nanomaterials from the substrate, which in turn decreases its activity. For example, after modified with 3-aminopropyltriethoxysilane, SiO_2, polyethylene glycol, or dextran, the peroxidase activity of Fe_3O_4 MNPs is decreased. Among the modifications, the dextran-coated Fe_3O_4 MNPs show the highest degree of activity. Usually, the modification's molecular thickness and weight are inversely correlated
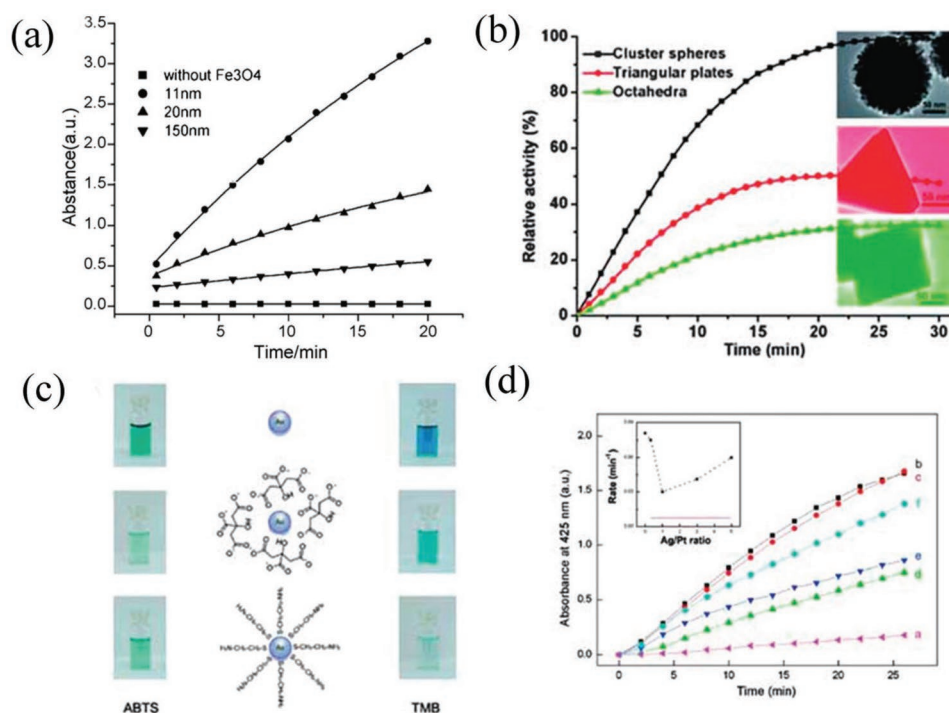
Figure 6. Tuning nanomaterials' peroxidase-like by controlling their a) size, b) shapes, c) surface modification, and d) alloying. a) Reproduced with permission.[175] Copyright 2008, Elsevier B.V. b) Reproduced with permission.[178] Copyright 2010, John Wiley & Sons. c) Reproduced with permission.[109] Copyright 2012, John Wiley & Sons. d) Reproduced with permission.[125] Copyright 2010, American Chemical Society.

with the activity. Unsurprisingly, a certain modification and coatings can improve the catalytic activity of the nanomaterials as well. For example, it has been exhibited that the Prussian blue modified Fe_2O_3 NPs with an enhanced peroxidase-like activity and it was correlated with modification levels, that is, a higher content of Prussian blue led to higher nanomaterial activity.

Nanomaterials with different surface charge modification and different substrates exhibit different peroxidase-like. Yang et al.[57] reported a comparison of peroxidase-like Fe_3O_4 MNPs with different modifications including citrate-modified, glycine-modified, polylysine-coated, poly(ethyleneimine)-coated, carboxymethyl dextran-coated and heparin-coated, to evaluate nanomaterial activity. The six Fe_3O_4 MNPs exhibited distinct surface charge, coating thickness, and charge intensity. With TMB as the substrate, anionic Fe_3O_4 MNPs had a high affinity and exhibited a high catalytic activity. The activity gradually increased when varying the zeta potential from positive to negative. With ABTS as the substrate, cationic Fe_3O_4 MNPs displayed a high affinity and subsequently a high peroxidase activity. The activity decreased dramatically in varying the zeta potential from positive to negative. These results revealed that a) the coating thickness is a contributing factor to the nanomaterial activity, and b) the charge characteristics of the modifications and the substrates play an important role in the activity. The use of interactions between the substrate and the coating to tune the nanomaterial's activity was also confirmed in several independent studies.[104,109,135,164]

Finally, surface modifications also have a great influence on the dispersibility and stability of nanomaterials, of which good dispersibility and stability are beneficial for improving affinity to substrates, catalysis velocity, and peroxidase-like activity. The lack of suitable surface capping ligands can affect the dispersibility and stability of nanomaterials, which in turn decreases the activity of the system. Therefore, it is highly important to find a balance between catalytic activity and stability.

4.4. Metal Doping and Alloying

The metal doping or alloying approaches also play critical roles in tuning nanomaterial's peroxidase-like catalytic activity. For instance, He et al.[125] reported the design of AgM (M = Au, Pb, Pt) bimetallic alloy nanostructures with tunable morphology and peroxidase-like activity (Figure 6d). Based on the reduction of two metal ions by a weak reductant, the AgM (M = Au, Pb, Pt) bimetallic alloy could designed to hollow/porous structures. AgM (M = Au, Pb, Pt) bimetallic alloy with suitable Ag/M ratios exhibits steady peroxidase-like activity. Furthermore, the catalytic activity of AgM (M = Au, Pb, Pt) bimetallic alloy can be fine-tuned by tuning the ratio of two metals, indicating another effective means to adjust the activity except for shape and size. The use of alloying method to adjust the nanomaterial's activity was also demonstrated in many other studies.[122,123]

Metal doping to improve the peroxidase-like activity of nanomaterial can be ascribed to three factors: a) metal doping cause the nanomaterial rich in surface defects such as oxygen vacancies and Ce^{3+} ions, which are active sites for the generation of ·OH radicals; b) the synergetic interaction between

metal and nanomaterial such as the strong redox behaviors of Ce^{3+}/Ce^{4+} and Fe^{2+}/Fe^{3+}; c) metal doping can also change the shape, size, surface area, and pore structures of nanomaterial to further tune the catalytic activity of nanomaterials. For example, Jampaiah et al.[88] reported a Fe-doped CeO_2 nanorods with enhanced peroxidase-like activity. Fe was chosen as a suitable dopant to modify CeO_2 nanorods, because it can induce more oxygen vacancies. Furthermore, their strong redox behaviors (Ce^{3+}/Ce^{4+} and Fe^{2+}/Fe^{3+}) and the synergetic interaction between them could also be an additional advantage for oxidation reactions. Besides, Song et al.[89] reported the Mo-doped CeO_2 NPs with enhanced peroxidase-like activity. The doped Mo not only causes more oxygen vacancies but also induce a smaller size and a bigger pore radius of Mo-doped CeO_2 NPs. The use of metal doping method to tune the nanomaterial's activity was also demonstrated in many other researches.[57,73,83]

4.5. Nanohybrids

Forming the composites is another effectively way to tune the peroxidase-like activity of nanomaterials. Nanocomposites combination of the respective performances of each component or to achieve cooperatively enhanced peroxidase-like activity. Moreover, nanocomposites usually bring novel functions and properties or promoted dispersibility and stability to further enhance intrinsic peroxidase-like activity of nanomaterials. Chen et al.[146] reported the graphene oxide–Fe_3O_4 magnetic nanocomposites with enhanced peroxidase-like activity. The graphene oxide not only promoted the dispersibility and stability of Fe_3O_4 MNPs, but as substrate absorbing species, which possess high surface-to-volume ratios show high affinity for substrates. The nanocomposites retain the magnetic properties and show an enhanced catalytic activity compared to bare Fe_3O_4 MNPs. Wang et al.[151] reported PtAg bimetallic nanoparticles-MoS_2 nanosheets with enhanced peroxidase-like activity. The PtAg-MoS_2 exhibits an enhanced catalytic activity than MoS_2 nanosheets alone. The enhanced peroxidase-like activity of PtAg-MoS_2 is attributed to the synergetic effects of MoS_2 nanosheets and PtAg bimetallic nanoparticles.

4.6. Other Factors

Like the HPR, the peroxidase-like activity of nanomaterials can also tune and affect by temperature and pH. Generally, the acidic condition and temperatures about 50–70 °C would be suitable for a peroxidase-mimicking activity of nanomaterials. However, the nearly neutral conditions and body temperature is acquired for the glucose detection.

5. Influence Factors of the Glucose Biosensor

In the last section, we summarized the tunable peroxidase-like activity of nanomaterials. In view of the glucose biosensor, we will emphasize on the factors influencing the biosensing aspect of the glucose detection in this part.

1. In the process of detection of glucose, the addition of GOx is needed to catalyze glucose generation of H_2O_2. Therefore, it can be influenced by pH, temperature, reaction times, etc. In addition, needing addition of excessive GOx are needed addition to catalyze glucose detection.

2. The sensitivity of glucose detection is influenced by the peroxidase-like activity of nanomaterials. Generally, the higher catalytic activity of nanomaterials exhibit lower detection limit for the glucose detection, thus driving us to explore the higher peroxidase activity of nanomaterials.

3. Most of the selectivity of the colorimetric glucose biosensor is dependent on the GOx, which catalyze glucose generation of H_2O_2. Fortunately, there is development of nonenzymatic colorimetric glucose biosensors. This glucose detection uses the "tandem nanozyme" and there is no need of adding GOx. Thus, the disadvantages of the enzyme can be avoided.

4. In real sample detection, the pretreatment of the samples can affect the accuracy of the detection consequence. In this process, some aspects must be paid attention to. For example, the spiking should be performed before the sample pretreatment and not after, in order to ensure that the whole method (which includes sample preparation in addition to measurement with the method) gives accurate results (evaluated based on the calculated recoveries). Moreover, the sample dilution factor during pretreatment needs to be considered and some authors overlook these aspects, in their eagerness to promote their research as alternative to current standard methods.

6. Conclusions, Challenges, and Perspectives

This review highlights the recent progress in nanomaterial-based peroxidase-like and its application for colorimetric glucose biosensor. The development history, mechanism, and colorimetric glucose biosensing of peroxidase-like of nanomaterials as well as tunable peroxidase-like of nanomaterials were discussed in detail. Compared with HPR, the nanomaterials exhibit flexibility in structure design and composition, easy separation and storage, high stability, simple preparation, and tunable catalytic activity. Although the above-mentioned advantages and great progress has been already made in nanomaterials, there are several challenges to be addressed.

1. Compared with HPR, the efficiency of most nanomaterials is still lower. Hence, the development of high catalytic activity nanomaterials will be a hot topic for future study. To some extents, additional surface modifications and coating can decrease the activity significantly, though the nanomaterial's core is highly active. Therefore, novel surface modification and coating techniques are needed to maximize the property of nanomaterials. Other methods such as metal doping and alloying, and composite are also awesome choices.

2. The peroxidase-like catalytic activity of nanomaterials was greatly influenced by the surface charge of nanomaterials with the substrates. Therefore, to evaluate the catalytic activity of nanomaterials, we should—according to surface charge—select appropriately substrates. In other words, can we explore new nanomaterials or new substrates to avoid this problem?

ADVANCED
SCIENCE NEWS
www.advancedsciencenews.com

NANO · MICRO
small
www.small-journal.com

3. Most of the reported peroxidase-like catalytic activity of nanomaterials require working in acidic conditions (pH < 6) rather than nearly neutral conditions (pH 6.0–7.4), which would restrict their practical applications. Therefore, the future challenges include improving the peroxidase-like catalytic activity for making it possess optimum catalytic activity in nearly neutral conditions.

4. Though selective detection tools have been developed for detection of glucose, the nanomaterials themselves have limited selectivity. Owing to the selectivity of glucose biosensor was mainly attributed to GOx, rather than the nanomaterials. Therefore, one of the greatest challenges to solve selectivity is to develop and design nanomaterials which possess high (asymmetric) selectivity toward given substrates.

5. Owing to their potential safety, environment, and health problems, there is a raising concern about the toxicity of nanomaterials from both public to the academia in recent years. To facing this challenge, apart from the nanomaterial itself, the surface coating and modification should also be considered. More efforts are required to transform the fundamental and leading scientific results to practical applications.

6. Recently, dual enzyme-like activities in nanomaterials (described as "tandem nanozyme") by incorporating glucose oxidase-like activity of AuNPs have drawn researcher attention. By utilizing the "tandem nanozyme," nonenzymatic glucose colorimetric detection systems (no need of adding glucose oxidase) have been successfully developed. However, the modification of protectors can inhibit the glucose oxidase-like activity of AuNPs. Thus, it requires new techniques to solve this problem or exploration of other superior "tandem nanozymes" to meet the requirements.

We hope that the readers gain some inspiration from this review and push further development of peroxidase-like activity of nanomaterials and its application for the glucose detection. And expect for more sensing tactics take part in this research field which create really workable biosensing devices serving for human world. We believe that the outlooks of peroxidase-like activity of nanomaterials and glucose biosensor will be bright in the present situation of research.

Acknowledgements

Conflict of Interest

The authors declare no conflict of interest.

[1] L. Zhao, F. Zhang, X. Ding, G. Wu, Y. Y. Lam, X. Wang, H. Fu, X. Xue, C. Lu, J. Ma, *Science* **2018**, *359*, 1151.

[2] D. Huang, X. Wang, C. Zhang, G. Zeng, Z. Peng, J. Zhou, M. Cheng, R. Wang, Z. Hu, X. Qin, *Chemosphere* **2017**, *186*, 414.

[3] C. Bommer, V. Sagalova, E. Heesemann, J. Manne-Goehler, R. Atun, T. Bärnighausen, J. Davies, S. Vollmer, *Diabetes Care* **2018**, *41*, dc171962.

[4] D. Huang, X. Qin, Z. Peng, Y. Liu, X. Gong, G. Zeng, C. Huang, M. Cheng, W. Xue, X. Wang, *Ecotoxicol. Environ. Saf.* **2018**, *153*, 229.

[5] E. J. Benjamin, S. S. Virani, C. W. Callaway, A. M. Chamberlain, A. R. Chang, S. Cheng, S. E. Chiuve, M. Cushman, F. N. Delling, R. Deo, S. D. de Ferranti, J. F. Ferguson, M. Fornage, C. Gillespie, C. R. Isasi, M. C. Jimenez, L. C. Jordan, S. E. Judd, D. Lackland, J. H. Lichtman, L. Lisabeth, S. Liu, C. T. Longenecker, P. L. Lutsey, J. S. Mackey, D. B. Matchar, K. Matsushita, M. E. Mussolino, K. Nasir, M. O'Flaherty, L. P. Palaniappan, A. Pandey, D. K. Pandey, M. J. Reeves, M. D. Ritchey, C. J. Rodriguez, G. A. Roth, W. D. Rosamond, U. K. A. Sampson, G. M. Satou, S. H. Shah, N. L. Spartano, D. L. Tirschwell, C. W. Tsao, J. H. Voeks, J. Z. Willey, J. T. Wilkins, J. H. Wu, H. M. Alger, S. S. Wong, P. Muntner, *Circulation* **2018**, *137*, e67.

[6] D. Huang, Z. Hu, Z. Peng, G. Zeng, G. Chen, C. Zhang, M. Cheng, J. Wan, X. Wang, X. Qin, *J. Environ. Manage.* **2018**, *210*, 191.

[7] Z. Yuan, F. J. Defalco, P. B. Ryan, M. J. Schuemie, P. E. Stang, J. A. Berlin, M. Desai, N. Rosenthal, *Diabetes, Obes. Metab.* **2018**, *20*, 582.

[8] R. Z. Wang, D. L. Huang, Y. G. Liu, C. Zhang, C. Lai, G. M. Zeng, M. Cheng, X. M. Gong, J. Wan, H. Luo, *Bioresour. Technol.* **2018**, *261*, 265.

[9] D. Huang, Z. Tang, Z. Peng, C. Lai, G. Zeng, C. Zhang, P. Xu, M. Cheng, J. Wan, R. Wang, *J. Taiwan Inst. Chem. Eng.* **2017**, *77*, 113.

[10] D. Huang, X. Qin, P. Xu, G. Zeng, Z. Peng, R. Wang, J. Wan, X. Gong, W. Xue, *Bioresour. Technol.* **2016**, *221*, 47.

[11] F. Xie, T. Liu, L. Xie, X. Sun, Y. Luo, F. Xie, T. Liu, L. Xie, X. Sun, Y. Luo, *Sens. Actuators, B* **2017**, *255*, 2794.

[12] D. L. Huang, R. Z. Wang, Y. G. Liu, G. M. Zeng, C. Lai, P. Xu, B. A. Lu, J. J. Xu, C. Wang, C. Huang, *Environ. Sci. Pollut. Res.* **2015**, *22*, 963.

[13] N. Hao, X. Zhang, Z. Zhou, R. Hua, Y. Zhang, Q. Liu, J. Qian, H. Li, K. Wang, *Biosens. Bioelectron.* **2017**, *97*, 377.

[14] R. Hua, N. Hao, J. Lu, J. Qian, Q. Liu, H. Li, K. Wang, *Biosens. Bioelectron.* **2018**, *106*, 57.

[15] F. Xie, X. Cao, F. Qu, A. M. Asiri, X. Sun, *Sens. Actuators, B* **2017**, *255*, 1254.

[16] D. Huang, X. Guo, Z. Peng, G. Zeng, P. Xu, X. Gong, R. Deng, W. Xue, R. Wang, H. Yi, *Crit. Rev. Biotechnol.* **2018**, *38*, 671.

[17] X. Liu, D. Huang, C. Lai, G. Zeng, L. Qin, C. Zhang, H. Yi, B. Li, R. Deng, S. Liu, Y. Zhang, *Trends Anal. Chem.* **2018**, *109*, 260.

[18] L. Qin, G. Zeng, C. Lai, D. Huang, P. Xu, C. Zhang, M. Cheng, X. Liu, S. Liu, B. Li, *Coord. Chem. Rev.* **2018**, *359*, 1.

[19] D. Huang, R. Deng, J. Wan, G. Zeng, W. Xue, X. Wen, C. Zhou, L. Hu, X. Liu, P. Xu, *J. Hazard. Mater.* **2018**, *348*, 109.

[20] Z. Zhou, N. Hao, Y. Zhang, R. Hua, J. Qian, Q. Liu, H. Li, W. Zhu, K. Wang, *Chem. Commun.* **2017**, *53*, 7096.

[21] Y. Song, W. Wei, X. Qu, *Adv. Mater.* **2011**, *23*, 4215.

[22] N. Hao, X. Zhang, Z. Zhou, J. Qian, Q. Liu, S. Chen, Y. Zhang, K. Wang, *Sens. Actuators, B* **2017**, *250*, 476.

[23] N. Hao, R. Hua, S. Chen, Y. Zhang, Z. Zhou, J. Qian, Q. Liu, K. Wang, *Biosens. Bioelectron.* **2018**, *101*, 14.

[24] C. Lai, X. Liu, L. Qin, C. Zhang, G. Zeng, D. Huang, M. Cheng, P. Xu, H. Yi, D. Huang, *Microchim. Acta* **2017**, *184*, 2097.

[25] L. Qin, G. Zeng, C. Lai, D. Huang, C. Zhang, P. Xu, T. Hu, X. Liu, M. Cheng, Y. Liu, *Sens. Actuators, B* **2017**, *243*, 946.

[26] N. Hao, J. Lu, Z. Zhou, R. Hua, K. Wang, *ACS Sens.* **2018**, *3*, 2159.

[27] D. Huang, X. Liu, C. Lai, L. Qin, C. Zhang, H. Yi, G. Zeng, B. Li, R. Deng, S. Liu, Y. Zhang, *Microchim. Acta* **2018**, *186*, 31.

[28] A. H. Valekar, B. S. Batule, M. I. Kim, K. H. Cho, D. Y. Hong, U. H. Lee, J. S. Chang, H. G. Park, Y. K. Hwang, *Biosens. Bioelectron.* **2017**, *100*, 161.

[29] B. Li, C. Lai, G. Zeng, L. Qin, H. Yi, D. Huang, C. Zhou, X. Liu, M. Cheng, P. Xu, C. Zhang, F. Huang, S. Liu, *ACS Appl. Mater. Interfaces* **2018**, *10*, 18824.

[30] B. L. Li, H. Q. Luo, J. L. Lei, N. B. Li, *RSC Adv.* **2014**, *4*, 24256.

[31] D. Huang, L. Liu, G. Zeng, P. Xu, C. Huang, L. Deng, R. Wang, J. Wan, *Chemosphere* **2017**, *174*, 545.

[32] L. Gao, J. Zhuang, L. Nie, J. Zhang, Y. Zhang, N. Gu, T. Wang, J. Feng, D. Yang, S. Perrett, X. Yan, *Nat. Nanotechnol.* **2007**, *2*, 577.

[33] X. Zhou, C. Lai, D. Huang, G. Zeng, L. Chen, L. Qin, P. Xu, M. Cheng, C. Huang, C. Zhang, C. Zhou, *J. Hazard. Mater.* **2018**, *346*, 113.

[34] J. Li, H. Hu, H. Li, C. Yao, *J. Mater. Sci.* **2017**, *52*, 10455.

[35] S. A. Zaidi, J. H. Shin, *Talanta* **2016**, *149*, 30.

[36] J. Wang, *Chem. Rev.* **2008**, *108*, 814.

[37] H. Wei, E. Wang, *Anal. Chem.* **2008**, *80*, 2250.

[38] D.-L. Huang, R.-Z. Wang, Y.-G. Liu, G.-M. Zeng, C. Lai, P. Xu, B.-A. Lu, J.-J. Xu, C. Wang, C. Huang, *Environ. Sci. Pollut. Res.* **2015**, *22*, 963.

[39] D. Huang, W. Xue, G. Zeng, J. Wan, G. Chen, C. Huang, C. Zhang, M. Cheng, P. Xu, *Water Res.* **2016**, *106*, 15.

[40] W. Xue, D. Huang, G. Zeng, J. Wan, C. Zhang, R. Xu, M. Cheng, R. Deng, *J. Hazard. Mater.* **2018**, *341*, 381.

[41] J. Xie, X. Zhang, H. Wang, H. Zheng, Y. Huang, J. Xie, *Trends Anal. Chem.* **2012**, *39*, 114.

[42] Y. Lin, J. Ren, X. Qu, *Acc. Chem. Res.* **2014**, *47*, 1097.

[43] H. Wei, E. Wang, *Chem. Soc. Rev.* **2013**, *42*, 6060.

[44] Q. Wang, H. Wei, Z. Zhang, E. Wang, S. Dong, *Trends Anal. Chem.* **2018**, *105*, 218.

[45] L. Su, W. Qin, H. Zhang, Z. U. Rahman, C. Ren, S. Ma, X. Chen, *Biosens. Bioelectron.* **2015**, *63*, 384.

[46] S. He, W. Shi, X. Zhang, J. Li, Y. Huang, *Talanta* **2010**, *82*, 377.

[47] Y. Fan, Y. Huang, *Analyst* **2012**, *137*, 1225.

[48] L. Su, J. Feng, X. Zhou, C. Ren, H. Li, X. Chen, *Anal. Chem.* **2012**, *84*, 5753.

[49] V. Figueroa-Espí, A. Alvarez-Paneque, M. Torrens, A. J. Otero-González, E. Reguera, *Colloids Surf. A* **2011**, *387*, 118.

[50] W. Shi, X. Zhang, S. He, Y. Huang, *Chem. Commun.* **2011**, *47*, 10785.

[51] D. Huang, C. Hu, G. Zeng, M. Cheng, P. Xu, X. Gong, R. Wang, W. Xue, *Sci. Total Environ.* **2016**, *574*, 1599.

[52] C. Hu, D. Huang, G. Zeng, M. Cheng, X. Gong, R. Wang, W. Xue, Z. Hu, Y. Liu, *Chem. Eng. J.* **2018**, *338*.

[53] M. Cheng, G. Zeng, D. Huang, C. Lai, P. Xu, C. Zhang, Y. Liu, *Chem. Eng. J.* **2016**, *284*, 582.

[54] C. Ding, Y. Yan, D. Xiang, C. Zhang, Y. Xian, *Microchim. Acta* **2015**, *183*, 625.

[55] N. V. S. Vallabani, A. S. Karakoti, S. Singh, *Colloids Surf., B* **2017**, *153*, 52.

[56] C.-J. Yu, C.-Y. Lin, C.-H. Liu, T.-L. Cheng, W.-L. Tseng, *Biosens. Bioelectron.* **2010**, *26*, 913.

[57] M. Hosseini, F. S. Sabet, H. Khabbaz, M. Aghazadeh, F. Mizani, M. R. Ganjali, *Anal. Methods* **2017**, *9*, 3519.

[58] K. Fan, H. Wang, J. Xi, Q. Liu, X. Meng, D. Duan, L. Gao, X. Yan, *Chem. Commun.* **2017**, *53*, 424.

[59] Y. Liu, M. Yuan, L. Qiao, R. Guo, *Biosens. Bioelectron.* **2014**, *52*, 391.

[60] Q. Liu, H. Li, Q. Zhao, R. Zhu, Y. Yang, Q. Jia, B. Bian, L. Zhuo, *Mater. Sci. Eng., C* **2014**, *41*, 142.

[61] R. Cui, Z. Han, J.-J. Zhu, *Chem. - Eur. J.* **2011**, *17*, 9377.

[62] Y. Song, X. Wang, C. Zhao, K. Qu, J. R. Dr, X. Q. Prof, *Chem. - Eur. J.* **2010**, *16*, 3617.

[63] Y. Guo, J. Li, S. Dong, *Sens. Actuators, B* **2011**, *160*, 295.

[64] Y. Guo, D. Liu, L. Jing, S. Guo, E. Wang, S. Dong, *ACS Nano* **2011**, *5*, 1282.

[65] Y. Song, K. Qu, C. Zhao, J. Ren, X. Qu, *Adv. Mater.* **2010**, *22*, 2206.

[66] R. Li, M. Zhen, M. Guan, D. Chen, G. Zhang, J. Ge, P. Gong, C. Wang, C. Shu, *Biosens. Bioelectron.* **2013**, *47*, 502.

[67] Y. Long, X. Wang, D. Shen, H. Zheng, *Talanta* **2016**, *159*, 122.

[68] W. Shi, Q. Wang, Y. Long, Z. Cheng, S. Chen, H. Zheng, Y. Huang, *Chem. Commun.* **2011**, *47*, 6695.

[69] B. Wang, F. Liu, Y. Wu, Y. Chen, B. Weng, C. M. Li, *Sens. Actuators, B* **2018**, *255*, 2601.

[70] D. Wu, X. Deng, X. Huang, K. Wang, Q. Liu, *J. Nanosci. Nanotechnol.* **2013**, *13*, 6611.

[71] X. Shan, L. Chai, J. Ma, Z. Qian, J. Chen, H. Feng, *Analyst* **2014**, *139*, 2322.

[72] S. Liu, J. Tian, L. Wang, Y. Luo, X. Sun, *RSC Adv.* **2012**, *2*, 411.

[73] J. Tian, Q. Liu, A. M. Asiri, A. H. Qusti, A. O. Al-Youbi, X. Sun, *Nanoscale* **2013**, *5*, 11604.

[74] T. Lin, L. Zhong, J. Wang, L. Guo, H. Wu, Q. Guo, F. Fu, G. Chen, *Biosens. Bioelectron.* **2014**, *59*, 89.

[75] L. Lin, X. Song, Y. Chen, M. Rong, T. Zhao, Y. Wang, Y. Jiang, X. Chen, *Anal. Chim. Acta* **2015**, *869*, 89.

[76] A. X. Zheng, Z. X. Cong, J. R. Wang, J. Li, H. H. Yang, G. N. Chen, *Biosens. Bioelectron.* **2013**, *49*, 519.

[77] H. Sun, A. Zhao, N. Gao, K. Li, J. Ren, X. Qu, *Angew. Chem., Int. Ed.* **2015**, *54*, 7176.

[78] C. Zhou, C. Lai, D. Huang, G. Zeng, C. Zhang, M. Cheng, L. Hu, J. Wan, W. Xiong, M. Wen, *Appl. Catal., B* **2018**, *220*, 202.

[79] D. Huang, Z. Li, G. Zeng, C. Zhou, W. Xue, X. Gong, X. Yan, S. Chen, W. Wang, M. Cheng, *Appl. Catal., B* **2019**, *240*, 153.

[80] C. Lai, M.-M. Wang, G.-M. Zeng, Y.-G. Liu, D.-L. Huang, C. Zhang, R.-Z. Wang, P. Xu, M. Cheng, C. Huang, H.-P. Wu, L. Qin, *Appl. Surf. Sci.* **2016**, *390*, 368.

[81] W. Chen, J. Chen, Y. B. Feng, L. Hong, Q. Y. Chen, L. F. Wu, X. H. Lin, X. H. Xia, *Analyst* **2012**, *137*, 1706.

[82] A. L. Hu, Y. H. Liu, H. H. Deng, G. L. Hong, A. L. Liu, X. H. Lin, X. H. Xia, W. Chen, *Biosens. Bioelectron.* **2014**, *61*, 374.

[83] A. P. Nagvenkar, A. Gedanken, *ACS Appl. Mater. Interfaces* **2016**, *8*, 22301.

[84] W. Chen, J. Chen, A.-L. Liu, L.-M. Wang, G.-W. Li, X.-H. Lin, *ChemCatChem* **2011**, *3*, 1151.

[85] X. Jiao, H. Song, H. Zhao, W. Bai, L. Zhang, Y. Lv, *Anal. Methods* **2012**, *4*, 3261.

[86] Q. Liu, Y. Yang, X. Lv, Y. Ding, Y. Zhang, J. Jing, C. Xu, *Sens. Actuators, B* **2017**, *240*, 726.

[87] Q. Liu, Y. Ding, Y. Yang, L. Zhang, L. Sun, P. Chen, C. Gao, *Mater. Sci. Eng., C* **2016**, *59*, 445.

[88] D. Jampaiah, T. Srinivasa Reddy, A. E. Kandjani, P. R. Selvakannan, Y. M. Sabri, V. E. Coyle, R. Shukla, S. K. Bhargava, *J. Mater. Chem. B* **2016**, *4*, 3874.

[89] X. Jiao, W. Liu, D. Wu, W. Liu, H. Song, *Anal. Methods* **2018**, *10*, 76.

ADVANCED
SCIENCE NEWS
www.advancedsciencenews.com

NANO · MICRO
small
www.small-journal.com

[90] H. Jia, D. Yang, X. Han, J. Cai, H. Liu, W. He, *Nanoscale* **2016**, *8*, 5938.

[91] J. Xie, Y. Huang, *Anal. Methods* **2011**, *3*, 1149.

[92] Q. Liu, R. Zhu, H. Du, H. Li, Y. Yang, Q. Jia, B. Bian, *Mater. Sci. Eng., C* **2014**, *43*, 321.

[93] J. Mu, Y. Wang, M. Zhao, L. Zhang, *Chem. Commun.* **2012**, *48*, 2540.

[94] L. Han, J. Shi, A. Liu, *Sens. Actuators, B* **2017**, *252*, 919.

[95] Z. Huang, J. Yang, L. Zhang, X. Geng, J. Ge, Y. Hu, Z. Li, *Anal. Methods* **2017**, *9*, 4275.

[96] R. Tian, J. Sun, Y. Qi, B. Zhang, S. Guo, M. Zhao, *Nanomaterials* **2017**, *7*, 347.

[97] G. Nie, L. Zhang, J. Lei, L. Yang, Z. Zhang, X. Lu, C. Wang, *J. Mater. Chem. A* **2014**, *2*, 2910.

[98] J. Sun, C. Li, Y. Qi, S. Guo, X. Liang, *Sensors* **2016**, *16*, 584.

[99] R. André, F. Natálio, M. Humanes, J. Leppin, K. Heinze, R. Wever, H. C. Schröder, W. E. G. Müller, W. Tremel, *Adv. Funct. Mater.* **2011**, *21*, 501.

[100] L. Han, L. Zeng, M. Wei, C. M. Li, A. Liu, *Nanoscale* **2015**, *7*, 11678.

[101] Q. Liu, Y. Yang, H. Li, R. Zhu, Q. Shao, S. Yang, J. Xu, *Biosens. Bioelectron.* **2015**, *64*, 147.

[102] T. Pirmohamed, J. M. Dowding, S. Singh, B. Wasserman, E. Heckert, A. S. Karakoti, J. E. King, S. Seal, W. T. Self, *Chem. Commun.* **2010**, *46*, 2736.

[103] J. Shah, R. Purohit, R. Singh, A. S. Karakoti, S. Singh, *J. Colloid Interface Sci.* **2015**, *456*, 100.

[104] Y. Jv, B. Li, R. Cao, *Chem. Commun.* **2010**, *46*, 8017.

[105] X. Jiang, C. Sun, Y. Guo, G. Nie, L. Xu, *Biosens. Bioelectron.* **2015**, *64*, 165.

[106] P. Ni, H. Dai, Y. Wang, Y. Sun, Y. Shi, J. Hu, Z. Li, *Biosens. Bioelectron.* **2014**, *60*, 286.

[107] G. L. Wang, L. Y. Jin, Y. M. Dong, X. M. Wu, Z. J. Li, *Biosens. Bioelectron.* **2015**, *64*, 523.

[108] D. Zeng, W. Luo, J. Li, H. Liu, H. Ma, Q. Huang, C. Fan, *Analyst* **2012**, *137*, 4435.

[109] S. Wang, W. Chen, A. L. Liu, L. Hong, H. H. Deng, X. H. Lin, *ChemPhysChem* **2012**, *13*, 1199.

[110] Y. J. Long, Y. F. Li, Y. Liu, J. J. Zheng, J. Tang, C. Z. Huang, *Chem. Commun.* **2011**, *47*, 11939.

[111] C. Jiang, J. Zhu, Z. Li, J. Luo, J. Wang, Y. Sun, *RSC Adv.* **2017**, *7*, 44463.

[112] H. Jiang, Z. Chen, H. Cao, Y. Huang, *Analyst* **2012**, *137*, 5560.

[113] M. N. Karim, S. R. Anderson, S. Singh, R. Ramanathan, V. Bansal, *Biosens. Bioelectron.* **2018**, *110*, 8.

[114] L. Jin, Z. Meng, Y. Zhang, S. Cai, Z. Zhang, C. Li, L. Shang, Y. Shen, *ACS Appl. Mater. Interfaces* **2017**, *9*, 10027.

[115] M. Ma, Y. Zhang, N. Gu, *Colloids Surf. A* **2011**, *373*, 6.

[116] Z. Gao, M. Xu, L. Hou, G. Chen, D. Tang, *Anal. Chim. Acta* **2013**, *776*, 79.

[117] K. Cai, Z. Lv, K. Chen, L. Huang, J. Wang, F. Shao, Y. Wang, H. Han, *Chem. Commun.* **2013**, *49*, 6024.

[118] T. G. Choleva, V. A. Gatselou, G. Z. Tsogas, D. L. Giokas, *Microchim. Acta* **2017**, *185*, 22.

[119] N. Wang, B. Li, F. Qiao, J. Sun, H. Fan, S. Ai, *J. Mater. Chem. B* **2015**, *3*, 7718.

[120] L. Hu, Y. Yuan, L. Zhang, J. Zhao, S. Majeed, G. Xu, *Anal. Chim. Acta* **2013**, *762*, 83.

[121] J. Liu, X. Hu, S. Hou, T. Wen, W. Liu, X. Zhu, J.-J. Yin, X. Wu, *Sens. Actuators, B* **2012**, *166–167*, 708.

[122] H. He, X. Xu, H. Wu, Y. Jin, *Adv. Mater.* **2012**, *24*, 1736.

[123] Y. Chen, H. Cao, W. Shi, H. Liu, Y. Huang, *Chem. Commun.* **2013**, *49*, 5013.

[124] X. Zhang, M. Wei, B. Lv, Y. Liu, X. Liu, W. Wei, *RSC Adv.* **2016**, *6*, 35001.

[125] W. He, X. Wu, J. Liu, X. Hu, K. Zhang, S. Hou, W. Zhou, S. Xie, *Chem. Mater.* **2010**, *22*, 2988.

[126] Y. Zhao, H. Qiang, Z. Chen, *Microchim. Acta* **2016**, *184*, 107.

[127] L. Han, C. Li, T. Zhang, Q. Lang, A. Liu, *ACS Appl. Mater. Interfaces* **2015**, *7*, 14463.

[128] F. Kang, X. Hou, K. Xu, *Nanotechnology* **2015**, *26*, 405707.

[129] A. Boujakhrout, P. Díez, P. Martínez-Ruíz, A. Sánchez, C. Parrado, E. Povedano, P. Soto, J. M. Pingarrón, R. Villalonga, *RSC Adv.* **2016**, *6*, 74957.

[130] M. Cui, J. Zhou, Y. Zhao, Q. Song, *Sens. Actuators, B* **2017**, *243*, 203.

[131] Q. Liu, P. Chen, Z. Xu, M. Chen, Y. Ding, K. Yue, J. Xu, *Sens. Actuators, B* **2017**, *251*, 339.

[132] J. Lei, X. Lu, G. Nie, Z. Jiang, C. Wang, *Part. Part. Syst. Charact.* **2015**, *32*, 886.

[133] J. Yu, X. Ma, W. Yin, Z. Gu, *RSC Adv.* **2016**, *6*, 81174.

[134] T. Lin, L. Zhong, L. Guo, F. Fu, G. Chen, *Nanoscale* **2014**, *6*, 11856.

[135] J. Yu, D. Ma, L. Mei, Q. Gao, W. Yin, X. Zhang, L. Yan, Z. Gu, X. Ma, Y. Zhao, *J. Mater. Chem. B* **2018**, *6*, 487.

[136] Y. Zhao, Y. Huang, J. Wu, X. Zhan, Y. Xie, D. Tang, H. Cao, W. Yun, *RSC Adv.* **2018**, *8*, 7252.

[137] X. Guo, Y. Wang, F. Wu, Y. Ni, S. Kokot, *Analyst* **2015**, *140*, 1119.

[138] K. Zhao, W. Gu, S. Zheng, C. Zhang, Y. Xian, *Talanta* **2015**, *141*, 47.

[139] Z. Dai, S. Liu, J. Bao, H. Ju, *Chemistry* **2009**, *15*, 4321.

[140] L. Zhang, M. Chen, Y. Jiang, M. Chen, Y. Ding, Q. Liu, *Sens. Actuators, B* **2017**, *239*, 28.

[141] L. Huang, W. Zhu, W. Zhang, K. Chen, J. Wang, R. Wang, Q. Yang, N. Hu, Y. Suo, J. Wang, *Microchim. Acta* **2017**, *185*, 7.

[142] T. Lin, L. Zhong, Z. Song, L. Guo, H. Wu, Q. Guo, Y. Chen, F. Fu, G. Chen, *Biosens. Bioelectron.* **2014**, *62*, 302.

[143] L. Zhang, L. Han, P. Hu, L. Wang, S. Dong, *Chem. Commun.* **2013**, *49*, 10480.

[144] X. Zuo, C. Peng, Q. Huang, S. Song, L. Wang, D. Li, C. Fan, *Nano Res.* **2009**, *2*, 617.

[145] Q. Li, G. Tang, X. Xiong, Y. Cao, L. Chen, F. Xu, H. Tan, *Sens. Actuators, B* **2015**, *215*, 86.

[146] Y. L. Dong, H. G. Zhang, Z. U. Rahman, L. Su, X. J. Chen, J. Hu, X. G. Chen, *Nanoscale* **2012**, *4*, 3969.

[147] Y. Wang, B. Zhou, S. Wu, K. Wang, X. He, *Talanta* **2015**, *134*, 712.

[148] S. Luo, Y. Liu, H. Rao, Y. Wang, X. Wang, *Anal. Biochem.* **2017**, *538*, 26.

[149] J. Chen, Q. Chen, J. Chen, H. Qiu, *Microchim. Acta* **2016**, *183*, 3191.

[150] Z. Sun, Q. Zhao, G. Zhang, Y. Li, G. Zhang, F. Zhang, X. Fan, *RSC Adv.* **2015**, *5*, 10352.

[151] S. Cai, Q. Han, C. Qi, Z. Lian, X. Jia, R. Yang, C. Wang, *Nanoscale* **2016**, *8*, 3685.

[152] J. Peng, J. Weng, *Biosens. Bioelectron.* **2017**, *89*, 652.

[153] L. Artiglia, S. Agnoli, M. C. Paganini, M. Cattelan, G. Granozzi, *ACS Appl. Mater. Interfaces* **2014**, *6*, 20130.

[154] F. Qiao, Q. Qi, Z. Wang, K. Xu, S. Ai, *Sens. Actuators, B* **2016**, *229*, 379.

[155] S. Kumar, P. Bhushan, S. Bhattacharya, *RSC Adv.* **2017**, *7*, 37568.

[156] G. Darabdhara, B. Sharma, M. R. Das, R. Boukherroub, S. Szunerits, *Sens. Actuators, B* **2017**, *238*, 842.

[157] H. Chen, Y. Li, F. Zhang, G. Zhang, X. Fan, *J. Mater. Chem.* **2011**, *21*, 17658.

[158] L. Zhang, X. Hai, C. Xia, X.-W. Chen, J.-H. Wang, *Sens. Actuators, B* **2017**, *248*, 374.

[159] X. Peng, G. Wan, L. Wu, M. Zeng, S. Lin, G. Wang, *Sens. Actuators, B* **2018**, *257*, 166.

[160] X. Tian, X. Wang, C. Dai, Y. Li, C. Yang, Z. Zhou, Y. Wang, *Sens. Actuators, B* **2017**, *245*, 221.

[161] Y. Ding, L. Sun, Y. Jiang, S. Liu, M. Chen, M. Chen, Y. Ding, Q. Liu, *Mater. Sci. Eng., C* **2016**, *67*, 188.

[162] Q. Liu, Y. Jiang, L. Zhang, X. Zhou, X. Lv, Y. Ding, L. Sun, P. Chen, H. Yin, *Mater. Sci. Eng., C* **2016**, *65*, 109.

[163] F. Yu, Y. Huang, A. J. Cole, V. C. Yang, *Biomaterials* **2009**, *30*, 4716.

[164] Y. Liu, F. Yu, *Nanotechnology* **2011**, *22*, 145704.

[165] H. Yi, D. Huang, L. Qin, G. Zeng, C. Lai, M. Cheng, S. Ye, B. Song, X. Ren, X. Guo, *Appl. Catal., B* **2018**, *239*, 408.

[166] L. Su, W. Dong, C. Wu, Y. Gong, Y. Zhang, L. Li, G. Mao, S. Feng, *Anal. Chim. Acta* **2017**, *951*, 124.

[167] M. Comotti, C. Della Pina, R. Matarrese, M. Rossi, *Angew. Chem., Int. Ed.* **2004**, *43*, 5812.

[168] X. Zheng, Q. Liu, C. Jing, Y. Li, D. Li, W. Luo, Y. Wen, Y. He, Q. Huang, Y. T. Long, C. Fan, *Angew. Chem., Int. Ed.* **2011**, *50*, 11994.

[169] W. Luo, C. Zhu, S. Su, D. Li, Y. He, Q. Huang, C. Fan, *ACS Nano* **2010**, *4*, 7451.

[170] D. Jiang, Q. Liu, K. Wang, J. Qian, X. Dong, Z. Yang, X. Du, B. Qiu, *Biosens. Bioelectron.* **2014**, *54*, 273.

[171] H. Zhang, X. Liang, L. Han, F. Li, *Small* **2018**, *14*, e1803256.

[172] K. Qu, P. Shi, J. Ren, X. Qu, *Chemistry* **2014**, *20*, 7501.

[173] Y. Lin, Z. Li, Z. Chen, J. Ren, X. Qu, *Biomaterials* **2013**, *34*, 2600.

[174] X. He, L. Tan, D. Chen, X. Wu, X. Ren, Y. Zhang, X. Meng, F. Tang, *Chem. Commun.* **2013**, *49*, 4643.

[175] F. F. Peng, Y. Zhang, N. Gu, *Chin. Chem. Lett.* **2008**, *19*, 730.

[176] K. N. Chaudhari, N. K. Chaudhari, J. S. Yu, *Catal. Sci. Technol.* **2011**, *2*, 119.

[177] J. W. Lee, H. J. Jeon, H. J. Shin, J. K. Kang, *Chem. Commun.* **2011**, *48*, 422.

[178] S. Liu, F. Lu, R. Xing, J.-J. Zhu, *Chem. - Eur. J.* **2011**, *17*, 620.

[179] S. Song, Y. Liu, A. Song, Z. Zhao, H. Lu, J. Hao, *J. Colloid Interface Sci.* **2017**, *506*, 46.

[180] A. K. Dutta, S. Das, S. Samanta, P. K. Samanta, B. Adhikary, P. Biswas, *Talanta* **2013**, *107*, 361.

[181] J. Mu, J. He, Y. Wang, *Talanta* **2016**, *148*, 22.

[182] A. K. Dutta, S. K. Maji, P. Biswas, B. Adhikary, *Sens. Actuators, B* **2013**, *177*, 676.

[183] N. Wang, J. Sun, L. Chen, H. Fan, S. Ai, *Microchim. Acta* **2015**, *182*, 1733.

[184] H. V. Tran, T. V. Nguyen, N. D. Nguyen, B. Piro, C. D. Huynh, *Microchim. Acta* **2018**, *185*, 270.

[185] Y. Zhang, Z. Zhou, F. Wen, J. Tan, T. Peng, B. Luo, H. Wang, S. Yin, *Sens. Actuators, B* **2018**, *275*, 155.

[186] D. Jampaiah, T. Srinivasa Reddy, V. E. Coyle, A. Nafady, S. K. Bhargava, *J. Mater. Chem. B* **2017**, *5*, 720.

[187] J. Wang, X. Yang, T. Wei, J. Bao, Q. Zhu, Z. Dai, *ACS Appl. Bio Mater.* **2018**, *1*, 382.